ACS NANO

www.acsnano.org

ARTICLE

Separation, Sizing, and Quantitation of Engineered Nanoparticles in an Organism Model Using Inductively Coupled Plasma Mass Spectrometry and Image Analysis

Monique E. Johnson,[*,†] Shannon K. Hanna,[‡] Antonio R. Montoro Bustos,[†] Christopher M. Sims,[‡] Lindsay C. C. Elliott,[§] Akshay Lingayat,[†,⊥] Adrian C. Johnston,[†,⊥] Babak Nikoobakht,[§] John T. Elliott,[‡] R. David Holbrook,[§] Keana C. K. Scott,[§] Karen E. Murphy,[†] Elijah J. Petersen,[‡] Lee L. Yu,[†] and Bryant C. Nelson[*,‡]

[†]Chemical Science Division, [‡]Biosystems and Biomaterials Division, and [§]Materials Measurement Science Division, Material Measurement Laboratory, National Institute of Standards and Technology, Gaithersburg, Maryland 20899, United States

Supporting Information

ABSTRACT: For environmental studies assessing uptake of orally ingested engineered nanoparticles (ENPs), a key step in ensuring accurate quantification of ingested ENPs is efficient separation of the organism from ENPs that are either nonspecifically adsorbed to the organism and/or suspended in the dispersion following exposure. Here, we measure the uptake of 30 and 60 nm gold nanoparticles (AuNPs) by the nematode, *Caenorhabditis elegans*, using a sucrose density gradient centrifugation protocol to remove noningested AuNPs. Both conventional inductively coupled plasma mass spectrometry (ICP-MS) and single particle (sp)ICP-MS are utilized to measure the total mass and size distribution, respectively, of ingested AuNPs. Scanning electron microscopy/energy-dispersive X-ray spectroscopy (SEM/EDS) imaging confirmed that traditional nematode washing procedures were ineffective at removing excess suspended and/or adsorbed AuNPs after exposure. Water rinsing procedures had AuNP removal efficiencies ranging from 57 to 97% and 22 to 83%, while the sucrose density gradient procedure had removal efficiencies of 100 and 93 to 98%, respectively, for the 30 and 60 nm AuNP exposure conditions. Quantification of total Au uptake was performed following acidic digestion of nonexposed and Au-exposed nematodes, whereas an alkaline digestion procedure was optimized for the liberation of ingested AuNPs for spICP-MS characterization. Size distributions and particle number concentrations were determined for AuNPs ingested by nematodes with corresponding confirmation of nematode uptake *via* high-pressure freezing/freeze substitution resin preparation and large-area SEM imaging. Methods for the separation and *in vivo* quantification of ENPs in multicellular organisms will facilitate robust studies of ENP uptake, biotransformation, and hazard assessment in the environment.

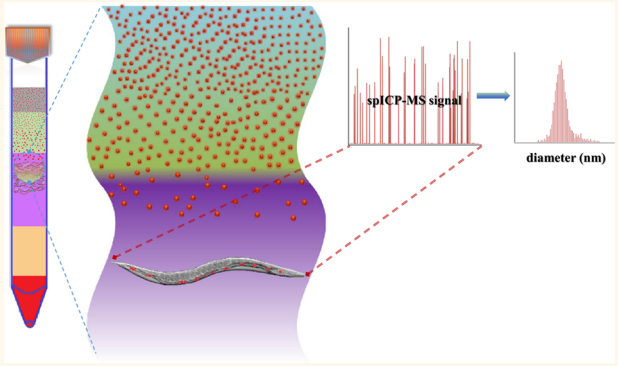

KEYWORDS: *single particle ICP-MS, nanotoxicity, Caenorhabditis elegans, uptake, gold nanoparticles, sucrose density gradient separation*

The rapid development of the nanotechnology industry has led to the increased incorporation of engineered nanoparticles (ENPs) into industrial materials and consumer products. As the manufacturing, use, and disposal of ENPs and ENP-enabled products expands, there is an increased likelihood that ENPs will be released into the environment (air, water, soils/sediments) and potentially affect ecologically relevant organisms. Hence, there is an urgent need to better understand the interaction between ENPs and environmental and biological systems. Accurate methods are necessary to quantify, characterize, and understand the interaction of ENPs with the environment and organisms.[1] Organisms such as cells, plants, aquatic species, and rodents are widely used in research

Received: September 29, 2016
Accepted: December 16, 2016
Published: December 16, 2016

DOI: 10.1021/acsnano.6b06582
ACS Nano 2017, 11, 526–540

Table 1. Techniques and Washing Procedures Used in *C. elegans* Nanomaterial Uptake Studies

ENPs	rinse procedure	quantification of uptake	visualization of uptake	approximate concentration found	ref
AgNPs	rinsed three times with M9 buffer	total Ag *via* ICP-MS	confocal microscopy	700−800 ng Ag/10000 *C. elegans*	Hunt *et al.*[15]
AgNPs	depuration followed by two rinses with EPA water	total Ag *via* ICP-MS	hyperspectral imaging, EDS analysis	≈300 ng Ag/mg *C. elegans*	Meyer *et al.*[42]
AgNPs	rinsed two times with water	NA	TEM/EDS, SEM, high-resolution microscopy	NA	Kim *et al.*[43]
CuONPs	rinsed five times with water	total Cu *via* ICP-MS	SRXRF	5.22 ± 0.63 μg Cu/g dry weight	Gao *et al.*[14]
AuNPs	rinsed three times with water	NA	optical microscopy	NA	Kim *et al.*[18]
CeO_2NPs	rinsed three times with moderately hard water	NA	hyperspectral imaging	NA	Arnold *et al.*[44]
FeOx colloids	no rinsing performed; 2 or 8 h depuration and molting	ferrozine assay	NA	0 h: 2.0 μg Fe/mg *C. elegans* 2 h: 1.0 μg Fe/mg *C. elegans* 8 h: 0.25 μg Fe/mg *C. elegans*	Hoss *et al.*[17]
AgNPs	2 h depuration, followed by three rinses with EPA water	total Ag *via* ICP-MS	NA	N2 wild-type: ≈40 ng Ag/mg *C. elegans* rme-1 strain: ≈75 ng Ag/mg *C. elegans* rme-6 strain: ≈20 ng Ag/mg *C. elegans* rme-1 strain: ≈30 ng Ag/mg *C. elegans*	Meyer *et al.*[45]

efforts designed to study potential toxic mechanisms related to ENPs. These model systems facilitate critical hazard/risk assessments that can inform sustainable production, use, and disposal of ENPs.[2,3]

Caenorhabditis elegans (*C. elegans*), a globally distributed, soil-inhabiting nematode species,[4] is a widely used multicellular organism model in multiple areas of biology[5] and is now becoming an important model in environmental toxicology[6] and in the chemical sciences.[7] This is attributed, in part, to its short maturation time (4 days), the large number of eggs/adult, well-defined cell lineage, availability of several genetically modified versions of the species, and its optical transparency.[8] Exposing *C. elegans* to environmental contaminants permits the observation of changes in physiology and behavioral effects, such as alterations in diet, locomotion, lifespan, reproduction, and morphology, allowing them to serve as a sentinel species for toxic substances.[9,10]

C. elegans has been extensively utilized in ENP-related toxicological studies[11] to investigate the potential biological effects of ENP exposure on organism health and behavior. Reported studies to date have mainly focused on metal and metal-oxide-based ENPs, which include studies on zinc oxide,[12,13] aluminum oxide,[13] titanium dioxide,[13] copper oxide,[14] silver (AgNPs),[15,16] iron oxide,[17] and gold (AuNPs).[18] In addition to toxicity measurements, there have also been several studies focused on characterizing the biodistribution of ingested ENPs.[13−15,17] This is important because the ENP concentration internalized by the organism may be a more relevant indicator of toxicity than the concentration in the exposure medium.[19] A wide range of approaches have been used to detect the uptake of ENPs in *C. elegans* including X-ray fluorescence[14] and dark-field hyperspectral imaging.[16] Within nanotoxicity studies, exposure concentrations of the ENPs often exceed environmentally relevant concentrations in order to induce a toxic response.[20−24] These high doses often hinder postexposure separation of organisms from exposure media, which hampers the acquisition of accurate quantitative information concerning ENP uptake. This fact is reflected in current *C. elegans* research approaches where only qualitative information on ENP uptake (*e.g.*, hyperspectral imaging, confocal imaging)[12,15,16] is typically reported. One technique that has been used to obtain both quantitative measurements of ENPs in suspension and uptake of metal and metal-oxide ENPs is inductively coupled plasma mass spectrometry (ICP-MS) because of its ability to provide total elemental mass concentrations and ENP size distribution measurements when operating in single particle ((sp)ICP-MS) mode.[25−29] Single particle ICP-MS has recently been used in a limited number of studies to measure the length of silver nanowires in *Daphnia magna* (*D. magna*) hemolymph,[30] the size of AuNPs in tomato plants,[31] and to size and quantify AgNPs in chicken meat,[32] ground beef,[33,34] and in the sediment oligochaete, *Lumbriculus variegatus*.[33,34] However, spICP-MS has not yet been applied to *C. elegans* for quantitative analysis, and it is unclear if NP extraction procedures from the aforementioned studies will work with *C. elegans* because of the tough nematode cuticle.[35]

In order to quantitatively measure and characterize uptake of ENPs, noningested ENPs must be separated from *C. elegans*. However, this separation process is complex, and to the best of our knowledge, there is no accepted or validated reference procedure describing how this separation should be performed. Procedures for removing excess ENPs from the nematode cuticle typically describe the use of either water or M9 (a buffer solution commonly used for *C. elegans* maintenance) rinses, followed by centrifugation to allow *C. elegans* to settle. Table 1 provides a comprehensive list of *C. elegans* uptake studies that have employed either a water or M9 washing procedure to rinse samples following exposure to ENPs. In each case, measurements were not provided describing the efficiency of the ENP removal process. Therefore, it is possible that the ENPs were nonspecifically attached to the nematodes' cuticles and/or associated with the *C. elegans* pellet throughout the washing process and not inherently ingested by the nematodes (*i.e.*, artifactual uptake).

Density gradient centrifugation has been widely employed as an ENP separation tool.[36−38] During centrifugation, high-density ENPs sediment at a rate faster than that of lower-

DOI: 10.1021/acsnano.6b06582
ACS Nano 2017, 11, 526−540

Scheme 1. Water Rinse Protocol: (A) *C. elegans* Exposed to AuNPs, (B) Sample Transfer, (C,D) Centrifugation, (E) Removal of Supernatant, (F) Three Water Rinses Followed by Centrifugation, and (G) Sample Transfer Followed by Lyophilization

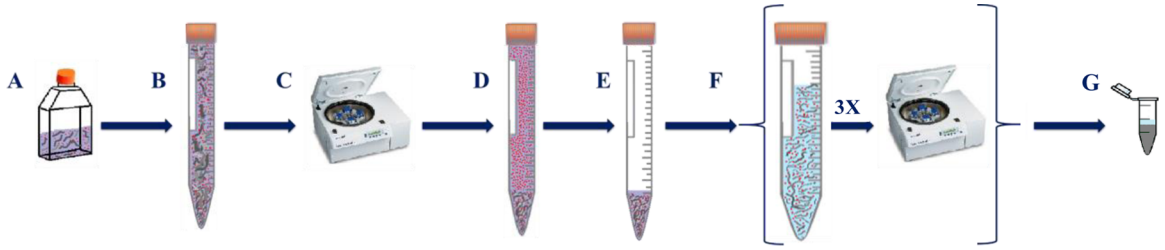

density ENPs, thus promoting localized separation of the ENPs within different density layers of the gradient. Recently, researchers in the Whitesides group[39] utilized isopycnic density gradient centrifugation with Percoll centrifugation medium to quantitatively measure mass density distributions in *C. elegans* populations. In addition, conventional sucrose density gradient centrifugation protocols are commonly used for separating viable *C. elegans* from bacteria, dead nematodes, and debris.[40,41] However, to our knowledge, density gradient centrifugation has not been developed nor applied toward the quantitative separation of multicellular organisms, such as *C. elegans*, from ENPs.

The objective of this work was to develop and optimize a robust methodology for quantifying and characterizing the total ingested mass and particle size distribution (PSD) of metallic ENPs internalized by *C. elegans*. To accomplish this, we employed a multidisciplinary approach which involved the development of a procedure based on isopycnic sucrose density gradient centrifugation to quantitatively separate the nematodes from AuNPs in an aqueous exposure model in concert with total Au mass analysis and AuNP PSD measurements *via* ICP-MS and spICP-MS analyses, respectively. We demonstrate that water rinsing alone followed by centrifugation of nematode samples is quantitatively inefficient for removing AuNPs remaining in the exposure suspension and/or from the *C. elegans*' cuticle. Sucrose density gradient centrifugation separations, on the other hand, were demonstrated to be analytically robust, reproducible, and quantitative for the removal of suspended or adsorbed ENPs.

RESULTS AND DISCUSSION

Comprehensive experiments were performed using National Institute of Standards and Technology (NIST) Reference Materials (RMs) 8012 and 8013 (nominally 30 and 60 nm AuNPs with mean diameters of 27.6 and 56.0 nm, respectively, as measured by transmission electron microscopy, TEM). Both RMs consist of aqueous suspensions of negatively charged, citrate-stabilized, monodispersed AuNPs with approximately spherical shape. An extensive characterization of the physicochemical properties of these AuNPs can be found in the NIST Reports of Investigation including analysis by TEM, scanning electron microscopy (SEM), nanoparticle tracking analysis, ICP-OES, and dynamic light scattering.[46,47] The major points of discussion will focus on the 60 nm AuNP-exposed samples, and 30 nm AuNP exposure data will be presented when relevant for experiment interpretation. *C. elegans* were exposed to both low and high AuNP concentrations, designated as LEx (40 ng/mL for 30 nm AuNPs and 333 ng/mL for 60 nm AuNPs) and HEx (100 ng/mL for 30 nm AuNPs and 835 ng/mL for 60 nm AuNPs), respectively. These concentrations were determined by a recent study which determined the annual predicated environmental concentrations of AuNPs in surface waters for the UK and US as 4.68 and 4.7 × 10^{-6} ng/mL, respectively.[48] The concentrations used in this study were several orders of magnitude higher than those predicted but still substantially lower than those often used in other nano-ecotoxicology studies which typically utilize concentrations near or above 1 mg/L.[49] Scheme 1 illustrates the traditional protocol for *C. elegans* AuNP exposure and postexposure sample processing. This approach utilizes water rinsing between centrifugation steps in an effort to remove cuticle-adsorbed AuNPs and AuNPs freely suspended in dispersion media. By following this scheme, the total ingested Au mass is overestimated due to incomplete removal of AuNPs in the suspension and/or to AuNPs nonspecifically adhered to the nematode cuticle. Figure 1A displays a SEM image of 60 nm AuNP-exposed nematodes (LEx) after sample processing *via*

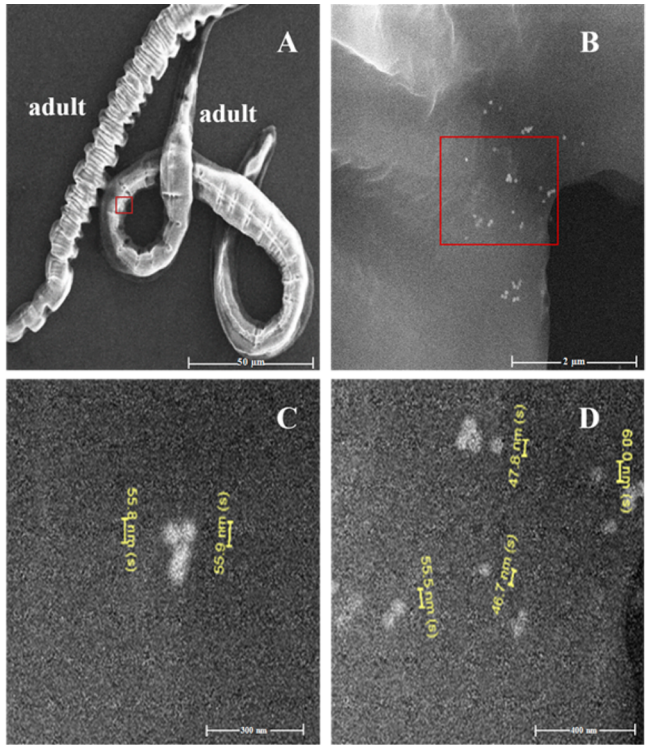

Figure 1. (A) Scanning electron microscopy image of adult *C. elegans* following exposure to 60 nm citrate-coated AuNPs (NIST); samples were acquired by Scheme 1. The area in the red inset is highlighted in (B). (B) Higher-magnification image of red inset in (A) revealed clusters of AuNPs on *C. elegans* cuticle. (C,D) Size analysis of cuticle-adsorbed particles found in the red inset in (B). Scale bars: (A) 50 μm, (B) 2 μm, (C) 300 nm, and (D) 400 nm.

DOI: 10.1021/acsnano.6b06582
ACS Nano 2017, 11, 526–540

Scheme 1. Higher-magnification images shown in Figure 1B–D, as well as in Figure 2, confirmed the presence of AuNPs on

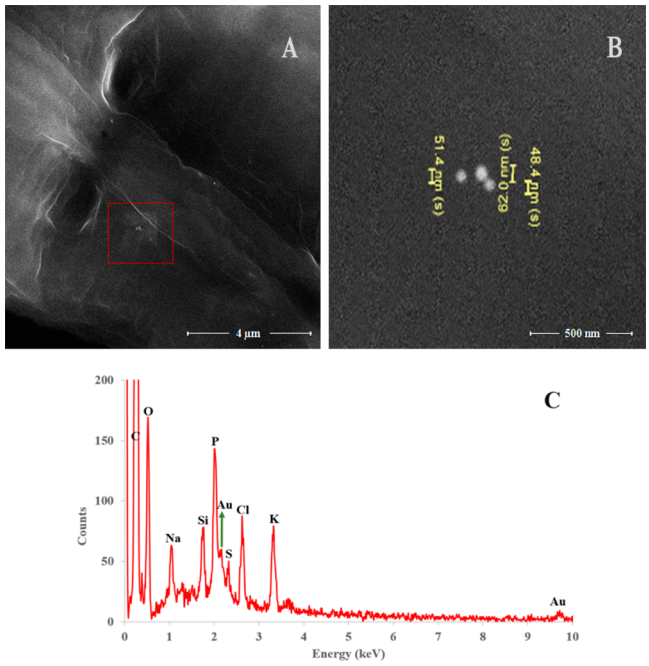

Figure 2. (A) High-magnification SEM image of the cuticle of the nematode in Figure 1. Sample was acquired by Scheme 1. (B) High-magnification of the high-contrast area in the red inset of (A). EDS analysis was performed on the area in red inset in (A). (C) Energy-dispersive X-ray spectrum of the area in the inset of (A). Note two peaks at 2.12 and 9.6 keV associated with the presence of elemental Au. Scale bars: (A) 4 μm and (B) 500 nm.

nematode cuticles. The red inset in Figure 1B, with size analysis shown in Figure 1C,D, displays individual AuNPs. Energy-dispersive X-ray spectroscopic (EDS) analysis, displayed in Figure 2C, of clusters of NPs on the cuticle of water-rinsed nematodes (similar to the clusters shown in Figures 1B and 2A) confirmed the presence of elemental Au. Note the presence of tight clusters of AuNPs (≈30 NPs) in a small area on the nematode cuticle (Figure 1B) with measured sizes (46.7–60.0 nm) consistent with the size distribution of NIST RM 8013 (47.0–65.4 nm; the spICP-MS measured size distribution of RM 8013 is shown in Figure S1).[47]

Additional SEM evidence demonstrating the ineffectiveness of water rinsing for the removal of AuNPs from nematode cuticles is also shown in Figures S2 and S3. SEM imaging employing a 0 and 15° stage tilt (Figure S3, with EDS analysis to confirm the presence of Au) provides a clearer view of cuticle-adsorbed AuNPs on two distinct sites of a rinsed nematode (Scheme 1). Commonly used analytical approaches, such as confocal microscopy (in scenarios where fluorescent particles are employed), and spICP-MS are not able to effectively discriminate whether AuNPs are internalized or surface-adsorbed. These results reflect the complexity and necessity of separating freely suspended ENPs from organisms after exposure and the critical need for the development of improved separation procedures.

Cuticle-adsorbed (not ingested) AuNPs would contribute a positive bias to the ICP-MS measurement of AuNP uptake by nematodes. Scheme 2 presents an alternative organism rinsing protocol, based on isopycnic sucrose density gradient centrifugation, for the quantitative separation of nematodes from AuNPs, which was specifically optimized to remove cuticle-adsorbed AuNPs and AuNPs suspended in culture media. A similar protocol, recently developed by our group, has been successfully applied for the separation of mixtures of AuNPs (varying sizes) in concert with spICP-MS.[50] This scheme facilitates the quantification and characterization of ENPs that are solely ingested by nematodes. The design of the sucrose density gradient layers within a centrifuge tube is illustrated in Figure S4 and constructed (from top to bottom of

Scheme 2. Sucrose Density Gradient Centrifugation Protocol: (A) *C. elegans* Exposed to AuNPs, (B) Sample Transfer, (C,D) Centrifugation, (E) Removal of Supernatant, (F) Two M9 Rinses Followed by Centrifugation, (G–I) Removal of Excess NPs by Sucrose Gradient Separation, (J) Three Water Rinses Followed by Centrifugation, and (K) Sample Transfer Followed by Lyophilization

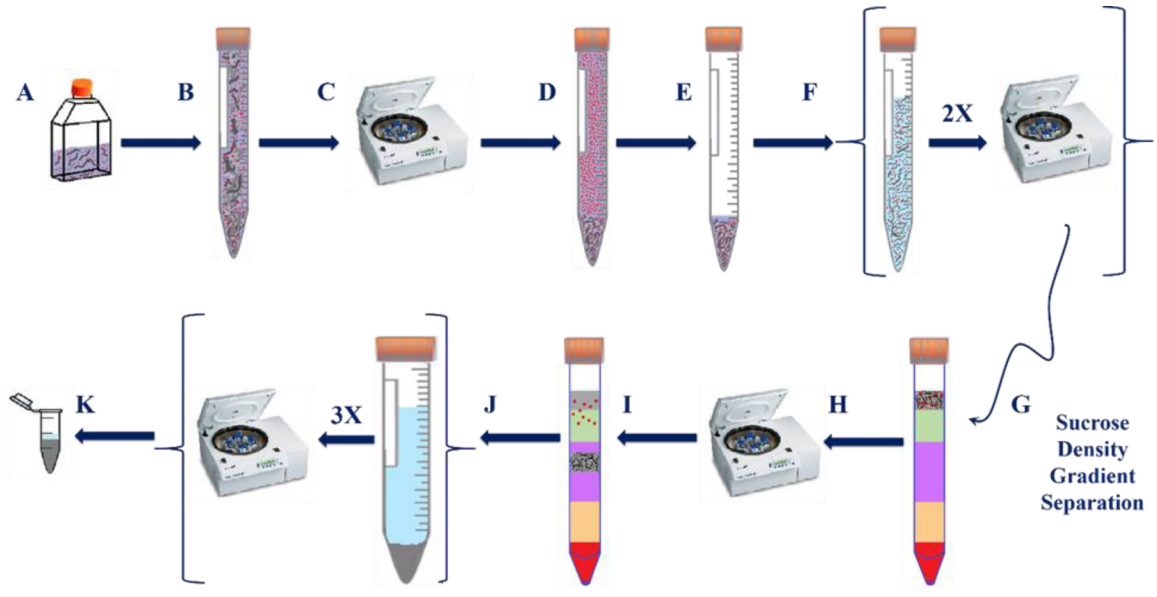

DOI: 10.1021/acsnano.6b06582
ACS Nano 2017, 11, 526–540

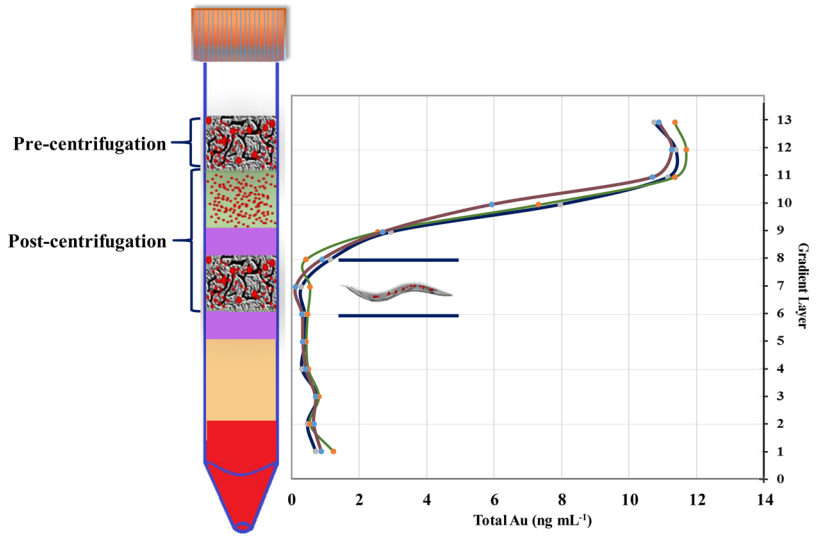

Figure 3. Distribution of Au from the sucrose density gradient centrifugal separation of *C. elegans* and 60 nm AuNP samples (n = 3) following 24 h exposure to 60 nm AuNPs (NIST). The nematode symbol depicted on the graph between the horizontal blue bars represents the nematode migration layer that was extracted after centrifugation (individual replicate data traces are represented by the colored lines where magnenta is sample 1, green is sample 2, and blue is sample 3).

the conical, plastic tube) as follows: 2 mL of AuNP-exposed nematode sample pellet, 2 mL of 100 μmol/L NaCl + [4 mL of 20% (w/v), 3 mL of 40% (w/v), and 2 mL of 50% (w/v)] sucrose. After centrifugation, nematodes in all sample treatment conditions settled between two interfaces: the interfaces between the NaCl layer (density 1.006 g/cm^3) and the 20% (w/v) sucrose layer and between the 20% (w/v) sucrose layer (density 1.081 g/cm^3) and the 40% (w/v) sucrose layer (density 1.176 g/cm^3). Nematodes may have separated into two layers *via* age (mixed-stage cultures were used for all exposure conditions) as the density of nematodes in a previous study ranged from 1.091 g/cm^3 for L1, L2, and L3 larvae to 1.074 g/cm^3 for adults.[39] The nematodes in these two layers were collected and processed completely *via* Scheme 2.

Three parallel experiments were devised to further characterize and also demonstrate the reproducibility of the sucrose density gradient separation mechanism (Scheme 2). In the first experiment, 2 mL aliquots of a nanosuspension containing both the 30 and 60 nm AuNPs (both at ~100 ng/mL) were transferred into centrifuge tubes containing sucrose gradients (n = 4). Following centrifugation, 1 mL aliquots of the gradient solution were successively removed, digested with 1 mL of aqua regia (HCl/HNO_3, 3:1, v/v), and analyzed for total Au content by conventional ICP-MS.[50] Total ICP-MS of the individual sucrose layers (data exhibited in Figure S5A and Table S1) revealed a swift decrease in Au concentration from the top to the bottom of the gradient. In fact, in reference to the colored gradient regions in Figure S4, an average sum of 1.8 ± 0.17, 2.3 ± 0.17, 15.7 ± 0.86, and 80.3 ± 0.96% of the Au measured was found in the 50% (w/v) sucrose section (indicated in red), 40% (w/v) sucrose section (indicated in yellow), 20% (w/v) sucrose section (indicated in purple), and the salt section (indicated in green), respectively.

In the second experiment, an equal volume fraction of nematodes (~50 000 nematodes/gradient) was added to an equal volume fraction of the nanosuspensions described in the first experiment, mixed for approximately 5 s, and 2 mL aliquots of this mixture were transferred into centrifuge tubes containing sucrose gradients (n = 4). Following centrifugation, 1 mL aliquots of the gradient solution were successively removed and processed as described in the first experiment. The nematodes in this gradient accumulated between gradient layers 4 and 6 (4–6 mL; Figure S5B and Table S2) in the centrifuge tube. An average sum of 83.6 ± 0.02% of the Au measured within the gradient was found between gradient layers 10–13 and an average sum of 2.4 ± 0.002% of the Au measured within the gradient was in the nematode migration layers (gradient layers 5–6).

In the third experiment, ~50 000 nematodes were exposed to 60 nm AuNPs (LEx) for 24 h (n = 3). Samples were processed from step A through step I of Scheme 2, after which 1 mL aliquots of the gradient solution were successively removed and processed for total Au content as described in the first experiment. An average sum of 88.7 ± 1.14% (Figure 3 and Table S3) of the Au measured within the gradient was found in gradient layers 9–13 (sample layer + salt layer). The nematodes in this experiment were found distributed across layers 6–8 (6–8 mL in the centrifuge tube; 20% (w/v) sucrose layer). The average sum of Au found in the nematode migration layers was 2.77 ± 0.21%, which represents the percentage of Au relative to the total Au mass fraction added to the gradient. Similar to the first two experiments, free AuNPs were predominately retained in the sample (gradient layers 11–13) and salt layers (gradient layers 9–11) of the gradient (Figure 3), while the nematodes moved down the gradient until they encountered the level of the sucrose density gradient that inhibited further movement (the average density of the nematodes closely matched the density of the 20% (w/v) sucrose layer in the sucrose gradient).[39]

It is reasonable to conclude that the AuNPs are retained in the sample and salt layers, as indicated in Figure S5A,B as well as in Tables S1–S3. It is also reasonable to conclude that the applied speed and time of centrifugation did not facilitate particle migration (to lower layers in the gradient), which allowed the separation of the nematodes from the AuNPs. In the proceeding steps of Scheme 2, following the separation of the nematodes from the AuNPs, the sucrose density gradient region in the centrifuge tube containing the live nematodes was

DOI: 10.1021/acsnano.6b06582
ACS Nano 2017, 11, 526–540

collected and rinsed with three additional aliquots of water to remove any residual Au. This additional washing step was also beneficial for removing excess sucrose from the nematode pellet prior to electron microscopy image analyses (below) and/or mass spectrometric elemental Au measurements. It is important to highlight that the relative contributions of the different steps in Scheme 2 were not quantified and that Scheme 2 did contain two additional washing steps compared to Scheme 1 in addition to the sucrose gradient centrifugation step.

SEM/EDS characterization was performed on the isolated 60 nm AuNP LEx nematode samples (see Exposure of Nematodes to AuNPs in the Experimental Section for details) to evaluate the efficiency of AuNP removal from the cuticle (Scheme 2). Two microliter nematode aliquots of the processed nematode pellet (each aliquot contained ≈40−50 nematodes) were transferred onto a Si wafer and allowed to air-dry overnight. Figure 4A shows a representative packet of dried nematodes,

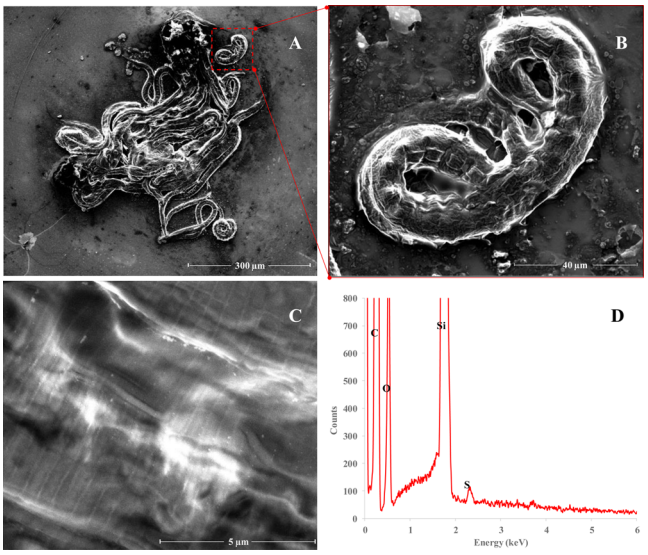

Figure 4. (A) Representative SEM image of a nematodes on a Si wafer following 24 h exposure to 60 nm AuNPs at 333 ng/mL with sample cleanup by sucrose density gradient centrifugation (scale bar: 300 μm). (B) High-magnification image of nematode in the red inset of (A) (scale bar: 40 μm). (C) Representative high-magnification image of the cuticle of a nematode exposed to 60 nm AuNPs (scale bar: 5 μm). The bright objects in (C) were presumed to be residual AuNPs on the surface of the nematode, which were subsequently analyzed by EDS (D). EDS did not reveal the presence of Au. A signal at 2.12 keV would indicate the presence of Au. C, O, Si, and S represent peaks for carbon (0.26 keV), oxygen (0.52 keV), silicon (1.75 keV), and sulfur (2.31 keV), respectively.

and Figure 4B is a magnified image of a single nematode shown in the red box inset in Figure 4A. Figure 4C displays a higher-magnification image of a representative nematode cuticle. A number of bright areas were observed on several nematode cuticles, and these were initially suspected to be adsorbed AuNPs. However, in all cases, EDS analyses of these bright spots (Figure 4D) could not conclusively confirm the presence of elemental Au. If Au was present, confirmatory signals would have been detected at 2.12 keV, but no signal was observed at this energy. More than 50 nematodes were surveyed and thoroughly inspected; neither the images nor EDS analyses indicated the presence of AuNPs. The bright spots observed on the nematode cuticles may instead be due to inorganic salt crystallites or organic deposits. Thus, the absence of AuNPs on the surveyed nematode cuticles confirmed the high separation efficiency of the sucrose gradient density centrifugation protocol.

Uptake of AuNPs. In order to quantitatively characterize, evaluate, and compare the efficiencies of the water rinsing (Scheme 1) and sucrose density gradient centrifugation procedures (Scheme 2), parallel 0 and 24 h AuNP uptake experiments were performed. These two time points represent the interaction period between AuNPs and nematodes in the exposure medium; the 0 h exposure period interaction was no longer than 10 s and accounts for immediate interaction between the nematodes and ENPs and takes into account the number of AuNPs that were either nonspecifically adsorbed onto the nematode cuticle or entrained within the sample pellet and not removed by the applied separation procedures (Scheme 1 or Scheme 2). During the sample cleanup process, the nematodes were kept at 4 °C (nematodes are largely immobilized at this temperature),[5] and so it is unlikely that the nematodes ingested significant amount of AuNPs. Additionally, it is highly improbable that AuNPs penetrated (absorbed) or were transported through the nematode cuticle as the cuticle is composed of heavily cross-linked collagens, insoluble cuticlins, glycoproteins, and lipids that make the cuticle impervious to the environment.[35] On the other hand, AuNP uptake data collected at the end of the 24 h exposure period are mainly representative of AuNPs specifically ingested by the nematodes, with a contribution from the AuNPs nonspecifically adsorbed onto the nematode cuticle at the 0 h time point. The relative contribution from nonspecific AuNP adsorption to the measured amount of AuNPs ingested depends upon which nematode processing scheme is applied to the sample.

Figure 5 shows the resulting ICP-MS uptake data from the 0 and 24 h (30 and 60 nm LEx and HEx exposure conditions) parallel uptake studies after nematode processing *via* Scheme 1 (Figure 5A,C) and Scheme 2 (Figure 5B,D), respectively. Au was not detected in nematodes processed by either scheme in the control exposure condition at either the 0 or 24 h time points. As shown in Figure 5A, nematode samples across all AuNP exposure conditions exhibited measurable amounts of Au at 0 h when Scheme 1 was utilized for postexposure nematode processing. In contrast, similar to control samples, nematodes from the 0 h exposure period for both the 30 nm LEx and HEx experiments were void of detectable Au when processed *via* Scheme 2 (Figure 5B). AuNPs were not completely removed by the sucrose density gradient process for the 60 nm LEx and HEx conditions, but Scheme 2 was far more efficient than Scheme 1 (95 and 85% reductions in Au mass, respectively) at removing nonspecifically cuticle-adsorbed and/or pellet-entrained AuNPs. After the 24 h exposure period, the amount of Au detected by ICP-MS increased considerably for both cleaning procedures (Figure 5A,B). Welch's unequal variance *t* test analyses were performed for each data set pair for each experiment (0 h *versus* 24 h exposure, water *versus* sucrose nematode processing). These analyses revealed the existence of an obvious dose−response trend for all of the nematode samples processed *via* Scheme 2 that is not evident for the nematodes exposed to the 60 nm LEx and HEx AuNP concentrations and processed *via* Scheme 1 (Figure 5A) at the 24 h time point. In particular, there is an unexpectedly low amount of Au uptake measured for the 60 nm HEx exposure sample that may be due to a measurement artifact; there exist no clear signs of measurement artifacts for samples processed

DOI: 10.1021/acsnano.6b06582
ACS Nano 2017, 11, 526−540

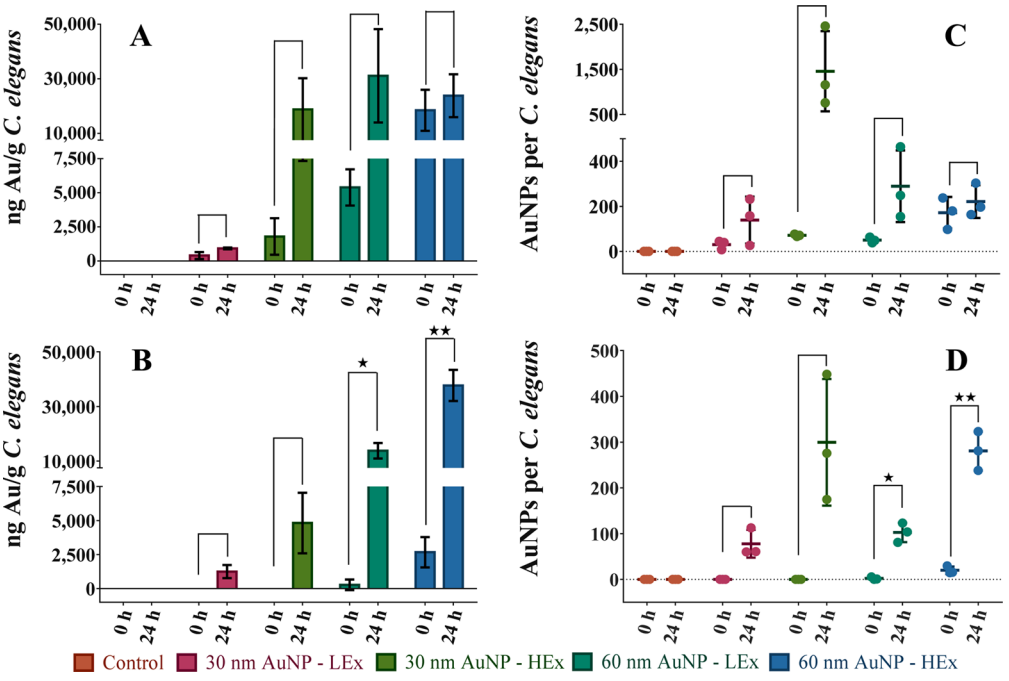

Figure 5. Uptake of AuNPs (reported as total ng Au/g *C. elegans via* ICP-MS analysis) in nematodes following 0 and 24 h exposure periods. Nematodes were exposed with media-only (control; no AuNPs), 30 nm AuNPs at 40 ng/mL (LEx) or 100 ng/mL (HEx), and 60 nm AuNPs at 333 ng/mL (LEx) or 835 ng/mL (HEx). (A,C) Total Au and the average calculated number of particles per *C. elegans* following postexposure sample cleanup by water rinsing (Scheme 1) and (B,D) postexposure sample processing by sucrose density gradient centrifugation (Scheme 2). Stars (*) indicate statistically significant increases in measured Au uptake levels after 24 h of AuNP exposure compared to 0 h of AuNP exposure using Welch's *t* test. One or two stars indicate $p < 0.05$ or 0.01, respectively. If no bar is shown in A or B, the Au signal was below the detection limit for the ICP-MS instrument and is recorded as a zero. All data points represent the mean of three independent measurements. Uncertainties (error bars) are 1 standard deviation, and horizontal bars in C and D are the means of the data points.

via Scheme 2. On the basis of the specified measurand (ng Au/g *C. elegans*), the lower than expected Au uptake for the 60 nm HEx condition could arise from either the measured Au uptake mass being too low, the measured nematode mass being too high, or a potential combination of these two factors. Of these, the measured nematode mass being too high is the most likely source of the measurement artifact. The 60 nm AuNPs are less stable in pure water than in the sucrose solution, meaning they are more likely to rapidly settle to the bottom of the centrifuge tube during the water washing/centrifugation steps (see Scheme 1, steps E and F, and compare to Scheme 2, sucrose separation steps I and J), where they can become entrained within the nematode pellet. This would result in the measured nematode mass being larger than its actual value (the measured nematode mass would be artifactually increased), resulting in a lower Au/nematode ratio. The 60 nm LEx condition would be less prone to this artifact due to the decreased amount of Au present in the system. Likewise, the 30 nm HEx condition would also be less prone to measurement error as the 30 nm AuNPs are less likely to settle to the bottom of the tube and become entrained within the nematode pellet compared to the 60 nm AuNPs.

The superior performance of the sucrose density gradient nematode processing method in comparison to the water-rinsing procedure can also be quantitatively described in terms of the absolute number of AuNPs accumulated by the nematodes. Using the total Au concentrations found in the 0 and 24 h experiments, and assuming a spherical particle shape and a defined particle diameter (TEM diameter of 27.6 ± 2.1 nm for the 30 nm AuNPs and 56.0 ± 0.5 nm for the 60 nm AuNPs listed in the NIST Reports of Investigation),[46,47] the average number of 30 and 60 nm AuNPs per nematode for all exposure conditions was calculated (see eqs 1, 2, and 3 in the Supporting Information for the calculation of these values) and illustrated in Figure 5C,D for Scheme 1 and Scheme 2, respectively. After correcting each 24 h AuNP/nematode result (subtracting the average number of AuNPs nonspecifically adsorbed to the cuticle or entrained within the sample pellet during the 0 h exposure period from the average number of AuNPs nominally ingested during the 24 h exposure period), we found that the AuNP/nematode results for the nematodes processed *via* Scheme 1 (41, 1387, and 239 AuNPs/nematode for the 30 nm LEx, 30 nm HEx, and 60 nm LEx AuNP exposures, respectively) were all higher than the average AuNP/nematode results calculated after processing the nematodes *via* Scheme 2 (78, 299, and 100 AuNPs/nematode for the 30 nm LEx, 30 nm HEx and 60 nm LEx AuNP exposures, respectively). The only exception to this pattern of uptake was the 60 nm HEx AuNP nematode exposure condition which had a lower average AuNP/nematode result for nematodes processed *via* Scheme 1 (49 AuNPs/nematode) in comparison to Scheme 2 (261 AuNPs/nematode). The singular 60 nm HEx AuNP/nematode finding using Scheme 1 may be a measurement artifact as alluded to previously. The uptake data obtained for the nematode samples processed *via* Scheme 2 did not show any obvious signs of measurement artifacts, and in fact, the data exhibited a clear dose–response trend (*i.e.*, concentration-dependent ENP uptake) in terms of AuNP uptake across all of the 30 and 60 nm AuNP exposure conditions (Figure 5D).

The measurement accuracy of the AuNP/nematode ICP-MS uptake data (Figure 5D) following postexposure sample

DOI: 10.1021/acsnano.6b06582
ACS Nano 2017, 11, 526–540

processing *via* Scheme 2 was independently evaluated by performing the same measurements using spICP-MS (Figure 6). Comparison of the indirect ICP-MS particle number

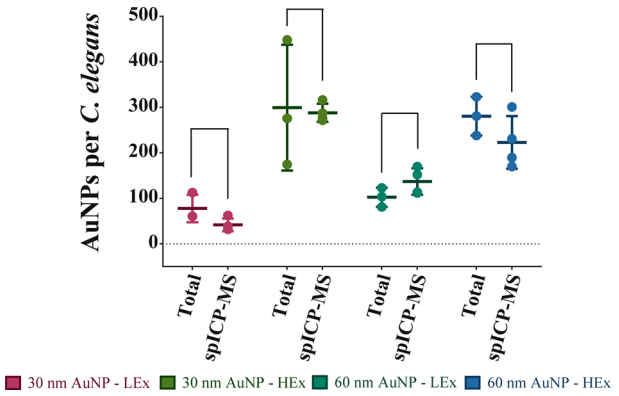

Figure 6. Comparison of the average number of particles per *C. elegans* as calculated by total Au analysis and spICP-MS following postexposure sample processing by sucrose gradient density centrifugation (Scheme 2). Welch's *t* test comparing the two independent analytical techniques found no significant difference between the means across all exposure conditions. A significant difference was found in the variances of the means for the 30 nm AuNP/HEx condition ($p < 0.05$; $p = 0.011$). Large horizontal bars are representative of the mean of the data points ($n = 3$ for total; $n = 4$ for spICP-MS), and the vertical lines with the short horizontal bars represent the standard deviations of the means.

measurements (total Au measurements converted to particle numbers) with the direct spICP-MS particle number measurements clearly demonstrated (Welch's unequal variances *t* test) that both instrumental methods measure equivalent levels of AuNPs/nematode and show the same increasing dose–response trends for the AuNP LEx and HEx exposure concentrations. However, data for samples in the 30 nm AuNP HEx condition had large variability, which precluded statistical significance. The reason(s) for the high variability in this one particular exposure condition is/are unclear. It is possible that a nonsystematic sample handling issue affected one of the three sample replicates (contamination within the digestion process or incomplete removal of the sucrose solution prior to sample lyophilization, *etc.*). However, further inspection of the data (comparison of 30 nm AuNP LEx *versus* 60 nm AuNP LEx and 30 nm AuNP HEx *versus* 60 nm AuNP HEx) suggests that the nematodes do not have a AuNP uptake size preference for particles at the nanoscale, at least for the AuNP range utilized in the present study. This is a key finding for future environmental nanotoxicology studies.

The results of the 0 h experiments and SEM analysis strongly suggest that the conventional practice of utilizing water rinsing followed by centrifugation to separate ENPs from nematodes, such as *C. elegans*, may not be an appropriate strategy for accurate measurements. Typically, sub-milligram/L ENP concentrations are used for nanouptake and nanotoxicity studies, but at the environmentally relevant exposure concentrations used for this study (sub-microgram/L), we found that a significant amount of nonassociated AuNPs was not adequately removed over the number of rinses typical for a *C. elegans* uptake study, and that the resulting data were of an unreliable quality. The use of sensitive analytical tools (such as ICP-MS or other techniques with excellent detection limits for metallic ENPs, but that are nonspecific in nature—*i.e.*, unable to visualize particulate matter) for whole-organism metrology requires that nonspecific adsorbance of ENPs to organism exoskeletons or cuticles be taken into account; otherwise, incorrect quantification of the ENP uptake is likely to occur. In the present study, AuNPs were not completely removed by the sucrose density gradient process for the 60 nm LEx and HEx conditions, but Scheme 2 was far more efficient than Scheme 1 in removing the nonspecifically adsorbed particles. Overall, internalized Au overestimations of 2 and 7% occurred for the 60 nm LEx and 60 nm HEx exposure condition when sucrose density gradient separation was employed as a washing step. This contrasts with the internalized Au overestimations of 43, 10, 17, and 78% that occurred for the 30 nm LEx, 30 nm HEx, 60 nm LEx, and 60 nm HEx exposure conditions, respectively, when water rinsing was employed to remove ENPs from nematode cuticles.

spICP-MS Analysis: Size Distributions of AuNPs in Water, Tetramethylammonium Hydroxide (TMAH), and Nematodes. Particle size distributions calculated from spICP-

Table 2. spICP-MS Measured Mode, Median, And Mean Particle Size of 30 and 60 nm AuNPs in Water, TMAH, and TMAH-Treated *C. elegans* Samples after 24 h Exposure

nanoparticles						
sample	TEM diameter (nm)[a]	matrix	mode (nm)	median (nm)	mean (nm)[b]	width (nm)[c]
30 nm AuNPs, NIST	27.6 ± 2.1	water	28.0	27.6	27.7 ± 2.0 (0.05)	2.9
		TMAH	27.3	27.6	27.2 ± 3.7 (0.05)	4.6
60 nm AuNPs, NIST	56.0 ± 0.5	water	56.0	56.0	56.0 ± 3.8 (0.09)	4.6
		TMAH	56.0	55.6	55.9 ± 6.4 (0.09)	8.0
C. elegans samples						
sample	TEM diameter (nm)[a]	matrix	mode (nm)	median (nm)	mean (nm)[b]	width (nm)[c]
30 nm LEx	27.6 ± 2.1	TMAH	34.8	35.0	38.4 ± 13.0 (0.44)	11.0[d]
30 nm HEx			33.3	35.2	38.5 ± 11.7 (0.14)	11.4[d]
60 nm LEx	56.0 ± 0.5		67.5	66.2	63.8 ± 11.7 (0.21)	6.7
60 nm HEx			69.2	67.1	65.9 ± 10.2 (0.16)	6.2

[a]Uncertainty values are the expanded uncertainties that account only for measurement replication. Expanded uncertainty values for TEM were determined in the NIST Reports of Investigation. Differences in expanded uncertainty could be attributed to different models used for each measurement technique and the number of particles analyzed. [b]Values are expressed as the calculated average, and the uncertainty, in parentheses, corresponds to one standard deviation (1σ) of the mean. [c]The width of the size distribution is defined as the distance between the 75th and the 25th percentiles of the particle diameters.[29] [d]Bimodal distribution as indicated in Figure 7.

DOI: 10.1021/acsnano.6b06582
ACS Nano 2017, 11, 526–540

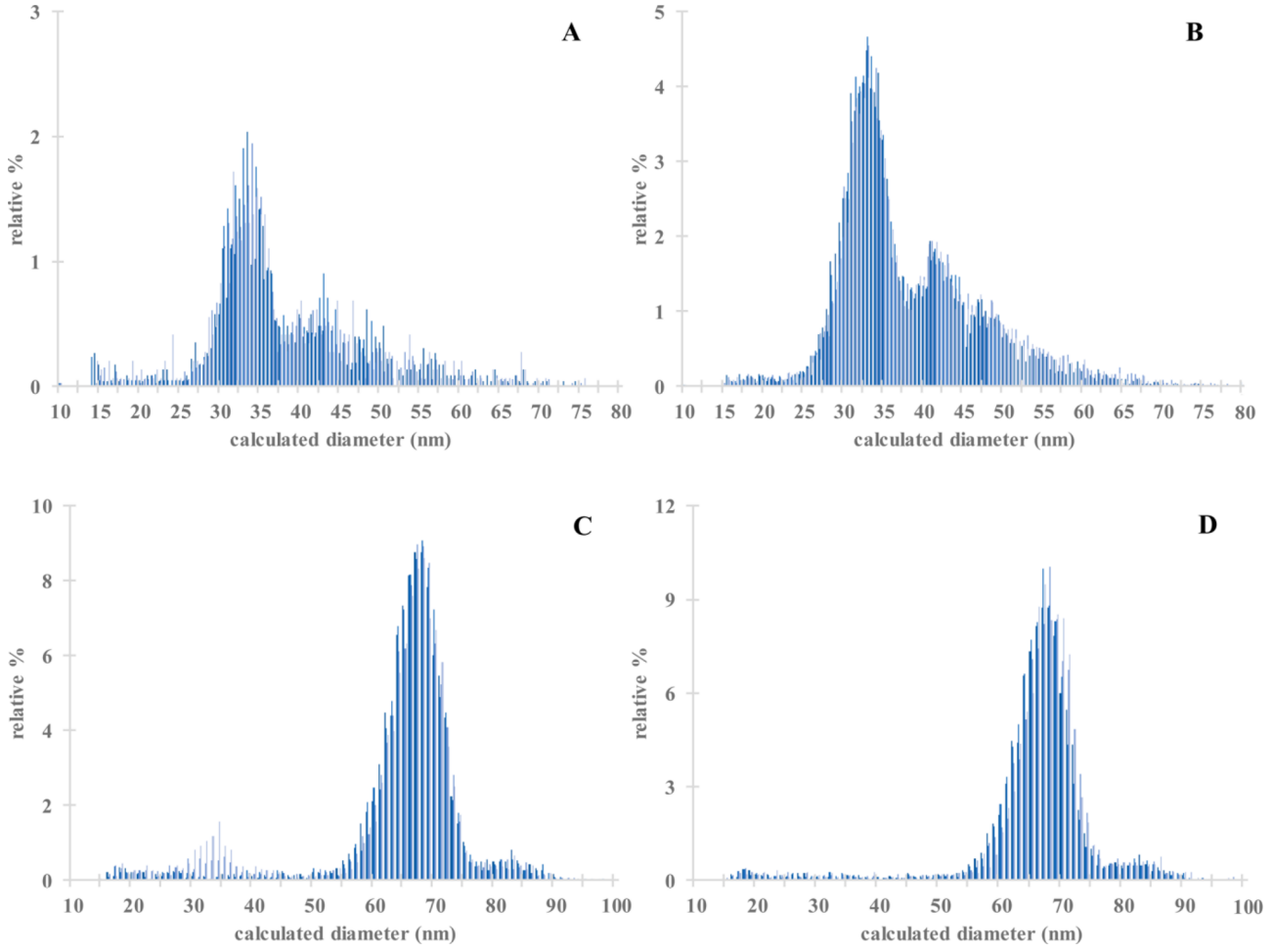

Figure 7. Overlayed PSDs of AuNPs extracted from nematodes using TMAH digestion after a 24 h exposure to NIST 30 nm AuNPs at (A) LEx exposure (n = 4) and (B) HEx exposure (n = 4) conditions, and NIST 60 nm AuNPs at (C) LEx exposure (n = 4) and (D) HEx exposure (n = 4) conditions. Mean diameters and standard deviations are given in Table 2.

MS measurements of AuNP suspensions in water showed good agreement with the particle sizes determined by TEM and reported on the Reports of Investigation for NIST RM 8012 and RM 8013 (data shown in Table 2 and Figures S6 and S1).[29,46,47] The details of the optimization of the TMAH digestion of AuNPs and biological tissues are discussed in the Supporting Information. Histograms exhibiting the size profiles of NIST RM 8012 and RM 8013 following treatment with TMAH are shown in Figure S7A,B. Similar to results previously reported by Gray *et al.*,[33,34] TMAH treatments did not have a substantial impact on the mean particle size for either AuNP. As shown in Table 2, the sizes (mean ± SD) were 27.7 ± 2.7 and 27.2 ± 3.6 nm, and 56.0 ± 4.0 and 55.9 ± 6.3 nm for the nominal 30 and 60 nm AuNPs in water and TMAH, respectively. However, there was a significant broadening in the width of the PSDs where the relative width increased by 52% for the 30 nm AuNPs and 74% for the 60 nm AuNPs when transitioning from analyzing the AuNPs in water to analyzing the AuNPs in TMAH. While we do not have a complete explanation for this phenomenon, we believe this broadening effect may be caused by the following factors: matrix effects[51] resulting from the 0.07% (w/w) TMAH and dissolution and subsequent recombination of NPs. Additional research to more fully understand this phenomenon is warranted.

Representative spICP-MS ^{197}Au time-resolved intensity data for nematodes in the control samples (data not shown) were similar to the time-resolved intensity data obtained for deionized water with an average detector response of 1.40 ± 0.12 counts (confirming that *C. elegans* are composed of little to no elemental Au). Nematodes were exposed for 24 h to 30 and 60 nm AuNPs using both LEx and HEx exposure conditions, processed *via* Scheme 2, and the ingested AuNPs were extracted from the nematodes using TMAH digestion. The PSD profiles for AuNPs extracted from the nematodes are presented in Figure 7 (AuNPs were detected for all exposure conditions). The AuNPs that were extracted from nematode samples were larger in diameter and had larger size distribution widths than the average PSD for pristine AuNPs. Notably, the AuNPs that were extracted from the 30 nm LEx and 30 nm HEx nematodes exhibited a bimodal PSD (Figure 7A,B). As shown in Table 2, the mean particle size increased from 27.2 to 38.4 and 38.5 nm for the 30 nm LEx and HEx exposure conditions, respectively, and from 55.9 to 63.8 and 65.9 nm for the 60 nm LEx and HEx exposure conditions (Figure 7C,D), respectively, when transitioning from analyzing pristine AuNPs in pure TMAH versus analyzing the AuNPs extracted from nematodes using TMAH tissue digestion. Note the broad PSDs for the AuNPs extracted from exposed nematodes in comparison to the PSDs for AuNPs in water or in TMAH.

DOI: 10.1021/acsnano.6b06582
ACS Nano 2017, 11, 526–540

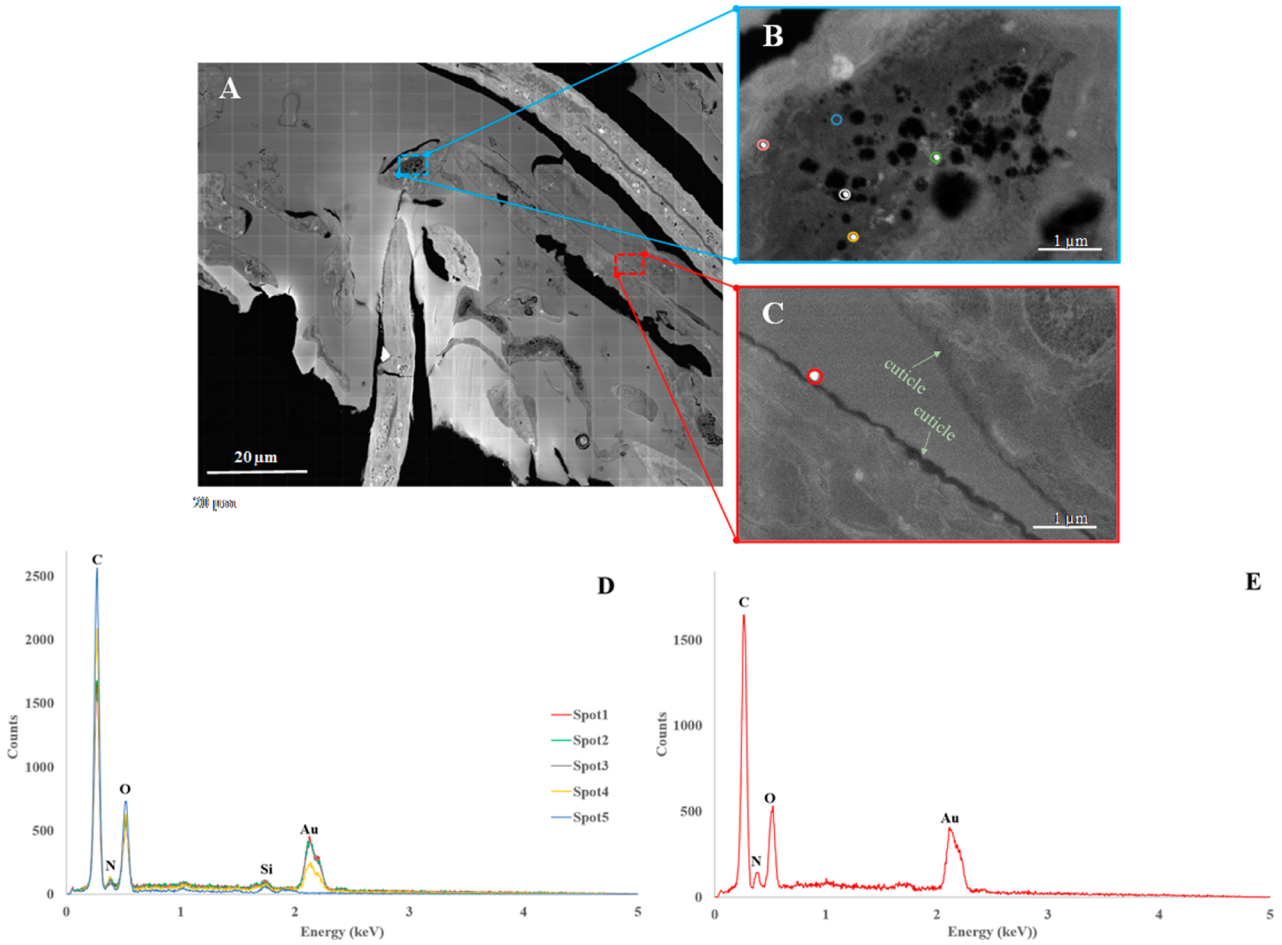

Figure 8. (A) Large-area SEM image of nematodes exposed to 60 nm AuNPs. Samples were acquired by Scheme 2. (B) Higher-magnification SEM image of blue inset highlighted in (A). (C) Higher-magnification SEM image of red inset highlighted in (A) displaying a AuNP adsorbed to *C. elegans* cuticle. (D) Energy-dispersive X-ray spectrum of four high-contrast areas (pink, white, yellow, and green circles) and a background reference area (red) (B) within the nematode sample. (E) Energy-dispersive X-ray spectrum of the high-contrast area on the nematode cuticle highlighted in (C). Note the high keV peaks at 2.12 associated with the presence of elemental Au. Scale bars: (A) 20 μm, (B) 1 μm, and (C) 1 μm.

The presence of significant levels of larger AuNPs in the PSD after nematode ingestion could be due to AuNP biotransformation through several different pathways. One pathway involves AuNP gut compaction and subsequent interaction with physiological fluid. Alternatively, the AuNPs could potentially aggregate in the intestine during the nematode's normal digestion process. The pH of the intestinal lumen ranges from pH ~6 in the anterior pharynx to pH 3.6 in the posterior intestine. The citrate coating that stabilizes the AuNPs may be stripped off in the acidic pH conditions during digestion, thus resulting in the occurrence of aggregation (as illustrated in Figure S8B).[52,53] Recently, Scanlan *et al.*[30] demonstrated that surface modifications to silver nanowires (AgNWs) occurred within the model organism *D. magna*, as AgNWs found in the hemolymph of *D. magna* were missing the oxide shell surrounding the silica coating. In all exposure cases, the finding of AuNPs larger than 45 nm for the 30 nm AuNP exposure conditions and 80 nm for the 60 nm AuNP exposure conditions was attributed to NP aggregation in the nematode gut tract. However, further experimental investigations are warranted in order to support this hypothesis. There is also potential evidence of digestion of the AuNPs within the *C. elegans* intestine as there is a large contribution of particles in the range of 15−40 nm for both the 60 nm LEx and HEx exposure conditions.

Large-Area SEM/EDS Imaging of AuNP-Exposed Nematodes. Visualization and confirmation of AuNPs within the digestive tract of the nematodes (*i.e.*, internalized AuNPs) were not feasible using conventional resin sample preparation techniques and SEM image analysis. Therefore, AuNP-exposed nematode samples processed *via* Scheme 2 were prepared for SEM imaging using high-pressure freezing and freeze substitution protocols. The resulting resin blocks were microtomed into 500 nm thin slices and subjected to large-area SEM imaging. The resulting images indicated that the ingested AuNPs were located primarily in the nematode intestine and intestinal lumen. Figure 8 shows characteristic SEM images of 60 nm AuNP LEx nematodes, where Figure 8A represents a large-area image. Figure 8B is a higher-magnification image of the blue box highlighted area in Figure 8A. Note the five circular spots, located in the *C. elegans* intestine, indicating four high-contrast areas and one background reference area. Figure 8C shows the occurrence of a AuNP adsorbed to a nematode cuticle (high-contrast area located in the red box in Figure 8A). EDS analysis confirmed the presence of Au in the four high-contrast areas in the

DOI: 10.1021/acsnano.6b06582
ACS Nano 2017, 11, 526−540

intestine (Figure 8D), as well as the AuNP on the nematode cuticle (Figure 8E).

The particle sizes for the AuNPs found in these characteristic samples ranged from 65 to 78 nm in diameter. Figure S8 displays evidence of AuNP aggregation (see Figure S8B, with EDS analysis, shown in Figure S8C, confirming the presence of Au in the red inset in Figure S8B) due to gut compaction of ENPs in the intestinal tract. This key finding strongly correlates with the spICP-MS data (Figure 7) showing broadened PSDs and larger mean particle sizes for AuNPs ingested by nematodes. This may also be evidence that the rigorous nature of TMAH digestion leads to disaggregation of particles that were potentially aggregated in the intestine of the nematodes. Figure S9 shows characteristic SEM images of 30 nm AuNP-HEx-exposed nematodes, and Figure S9A presents a large-area image. Figure S9B shows a higher-magnification area of the nematode intestine in Figure S9A. Only a single area of high contrast was found near the microvilli of the intestine, and it was later confirmed to be a AuNP by EDS analysis (Figure S9C). It is conceivable that this dearth of internalized 30 nm AuNPs is due to the NPs having been dislodged during the microtoming procedure. Additional evidence of internalized AuNPs, with elemental Au confirmation *via* EDS, is provided in Figure S10. Translocation of AuNPs from the intestine to other cellular compartments was not observed in the present exposure study, and this may be due to the relatively short (24 h) incubation period.

CONCLUSION

Invertebrate model organisms, such as *C. elegans*, are increasingly utilized as alternative *in vivo* systems to vertebrate model organisms, such as rodents, to investigate the uptake, translocation, transformation, and potential toxicity of ENPs in the environment. Thus far, no standardized protocols exist for evaluating the uptake of ENPs in whole organisms. Standardized protocols are essential for establishing the validity and reproducibility of ecotoxicity and/or risk assessments. The present research describes a quantitative protocol for evaluating the uptake of AuNPs in *C. elegans*, with particular emphasis on mitigating the effects of measurement artifacts such as ENP cuticle adsorption that naturally occur during nematode exposures and that may occur during sample preparation. The development and optimization of the sucrose density gradient centrifugation protocol for the specific removal and separation of cuticle-adsorbed AuNPs permitted reliable quantitative measurement of 30 and 60 nm AuNP uptake and potential biotransformation (gut tract aggregation) within live nematodes using spICP-MS. Limitations of this method that could lead to underestimations in the number of particles ingested by nematodes include factors such as (1) the potential for organisms to excrete ingested particles during the separation process after the exposure period and (2) the presence of dauer nematodes (that do not ingest NPs) that arise from culturing in non-optimal liquid media conditions adding to the nematode mass. Also, the sucrose density gradient centrifugation protocol as currently implemented cannot be easily utilized to separate ENPs from organisms exposed to exceedingly high amounts of ENPs (*e.g.*, >24 × 10^6 60 nm AuNPs/L) without applying multiple cycles of the sucrose density gradient or scaling up Scheme 2 (*i.e.*, size of the centrifuge tubes, volume of sucrose, *etc.*). spICP-MS analysis of AuNPs currently has a size detection limit of approximately 10 nm[54] that restricts its utility in nanouptake studies for AuNPs smaller than 10 nm. Further instrumental improvements will extend its applicability to smaller NP sizes. In the present study, there was no significant change in the PSD of AuNPs after TMAH treatment, thus changes in the PSDs of the ingested AuNPs can reasonably be attributed to transformations of bioaccumulated AuNPs after digestion by the nematodes. It is also possible that TMAH could disaggregate AuNPs previously ingested by nematodes,[33,34] but this was not clear in our investigation. In summary, the newly developed ENP/whole-organism separation methodology, in combination with single particle uptake measurements, merits consideration as a standardizable platform for reducing the measurement variability and sampling bias that can occur in environmental nanotoxicology studies. The techniques described in this report should be immediately beneficial for improving ENP hazard and risk assessments in the environment.

EXPERIMENTAL SECTION

Nematode Maintenance. *C. elegans* nematodes (wild-type, Bristol strain, N2) and *Escherichia coli* (*E. coli*) OP50 were purchased from the Caenorhabditis Genetics Center (CGC, University of Minnesota). Nematodes were cultured on NGM plates seeded with *E. coli* (OP50) at 20 °C. Once the bacterial lawn was cleared, gravid nematodes were washed off plates and cultured in S-basal liquid media (S-basal complete/500 mL: contains 0.5 mL of cholesterol in ethanol (5 mg/mL), a mineral mixture, 1.5 mL of 1 M $MgSO_4$, 1.5 mL of 1 M $CaCl_2$, 5 mL of penicillin−streptomycin, and 2.5 mL of amphotericin B).[40,41] Live/viable nematodes were then separated from bacteria, dead nematodes, and debris by a sucrose density gradient centrifugation protocol described by Lewis and Fleming,[40,41] resulting in L3, L4, and adult nematodes. Briefly, nematodes were resuspended in 15 mL of cold 100 μmol/L NaCl and mixed by inversion. An equal volume fraction of cold sucrose (60%, w/v) was then added to the tube (without any additional agitation), and finally, an additional 5 mL of NaCl was gently added to the top of this mixture. The nematode/bacteria mixture was then transferred to a swinging bucket centrifuge and spun for 5 min at 72*g*. Nematodes at the interface of the salt and sucrose mixture were transferred to a centrifuge tube, and excess salt and sucrose were rinsed by centrifugation. Mixed-stage nematodes were resuspended, and the number of nematodes in twelve 2 μL droplets were counted under a light microscope and averaged for an estimation of total population density.

Exposure of Nematodes to AuNPs. Using approximately 250 000 nematodes/exposure condition, the required dilutions in S-basal complete were prepared with a target total volume of 50 mL/replicate (nematodes + exposure media + AuNPs). S-basal complete media and nematodes were distributed into 25 cm^2 tissue culture flasks (n = 3 for nonexposed, 30 nm AuNP, and 60 nm AuNP exposure conditions). The appropriate volumes of stock AuNPs were pipetted into flasks, capped and inverted three times, and mixed gently with an electronic pipet for 5 s (to ensure complete dispersion of the ENPs), and then 25 mL of the nematode/media/AuNP mixture was immediately transferred to a centrifuge tube and placed on ice. These replicates were regarded as the "0 h exposure" conditions and were cleaned by the protocols stated below. The remaining 25 mL sample in the tissue culture flask was placed on a shaker in an incubator at 20 °C for 24 h and then processed by the sample cleanup protocols described below. These samples are designated as the "24 h exposure" condition. For nonexposed nematodes (controls), 1 mL of deionized water was added to . Two concentration levels were chosen and were designated as the "low concentration exposure, LEx" and "high concentration exposure, HEx" level, respectively. For each exposure level, equal particle number concentrations of 30 and 60 nm AuNPs were used. For the LEx condition, Au concentrations of 40 ng/mL (30 nm AuNPs) and 333 ng/mL (60 nm AuNPs) corresponded to a particle number concentration of 1.9 × 10^{11} per exposure. For the HEx condition, Au concentrations of 100 ng/mL (30 nm AuNPs) and

DOI: 10.1021/acsnano.6b06582
ACS Nano 2017, 11, 526−540

835 ng/mL (60 nm AuNPs) corresponded to a particle number concentration of 4.7×10^{11} particles per exposure.

Postexposure Sample Treatment and AuNP Cleanup. Two different nematode cleanup procedures were employed for the separation of nematode populations from nonassimilated AuNPs: a traditional water rinse (Scheme 1) and sucrose density gradient centrifugal separation (Scheme 2). In cleanup Scheme 1, control and AuNP-exposed samples were transferred into centrifuge tubes and spun at 1870*g* for 5 min. The supernatant was removed by vacuum filtration, and the remaining nematode pellet was rinsed three times with 50 mL of 4 °C deionized water followed by centrifugation at 1870*g* for each rinse. The remaining pellet was transferred into a 1.5 mL microcentrifuge tube and lyophilized for 24 h. For Scheme 2, 20, 40, and 50% sucrose solutions were made by dissolving the appropriate amount of sucrose in deionized water. Sucrose solutions were gently heated, stirred until completely dissolved, and stored at 4 °C. Food coloring was added as a visual aid to discriminate the different concentrations of sucrose as well as to better visualize nematode layers after centrifugation. The sucrose density gradient separation column was carefully constructed from top to bottom, using a 15 mL plastic centrifuge tube as follows: 2 mL of 100 μmol/L NaCl, 20% sucrose (4 mL, w/v), 40% sucrose (3 mL, w/v), and 50% sucrose (2 mL, w/v). Control and AuNP-exposed nematode samples were rinsed twice with 25 mL of M9 buffer (3 g of KH_2PO_4, 6 g of Na_2HPO_4, 5 g of NaCl, and 1 mL of $MgSO_4$ in 1 L) and kept in an ice bath until the sucrose density gradient centrifuge columns were prepared. The nematode samples (~1.5 mL) were gently added, using a pipet, to the top of the gradient. Centrifugal separation of nematodes from AuNPs was performed at 4 °C in a swinging bucket centrifuge under the following conditions: 5 min at 172*g* immediately (*i.e.*, without interruption) followed by 5 min at 1254*g*. Figure S5B is representative of nematode samples within the gradient prior to and after centrifugation. Prior to centrifugation (denoted by the "pre-centrifugation" label), nematodes rest on top of the interface between the salt layer and the 20% sucrose layer immediately after the nematodes are added to the gradient. After centrifugation (denoted by the "post-centrifugation" label), nematodes in all sample treatment conditions settle between two interfaces: the interfaces between the NaCl layer (density = 1.006 g/cm^3) and the 20% (w/v) sucrose layer and between the 20% (w/v) sucrose layer (density = 1.081 g/cm^3) and the 40% (w/v) sucrose layers (density = 1.176 g/cm^3). The nematodes were removed by pipet from the gradient and rinsed an additional three times (spun at 1870*g* for 5 min) with 50 mL of ice-cold deionized water to remove excess sucrose prior to 24 h lyophilization. Lyophilized samples were stored in a desiccator prior to digestion and subsequent analysis.

Three parallel experiments were designed to investigate the efficacy of the AuNP/*C. elegans* separation. In the first experiment, 2 mL of a nanosuspension containing 30 and 60 nm AuNPs (both at ~100 ng/mL; citrate-stabilized, NIST) was transferred into centrifuge tubes containing sucrose gradients (n = 4). In the second experiment, an equal volume fraction of nematodes (~50 000 nematodes/gradient) was added to an equal volume fraction of the aforementioned nanosuspension, mixed for approximately 5 s, and 2 mL of this mixture was transferred into centrifuge tubes containing sucrose gradients (n = 4; construction of the gradient is illustrated in Figure S4). In the third experiment, nematodes (~50 000 nematodes) were exposed to 60 nm AuNPs (LEx) for 24 h. Samples were then processed from step A through step I of Scheme 2. After step I, 1 mL aliquots (out of a total of 13 mL) of the gradient solution were successively removed. For total Au analysis of all sucrose gradient layers, these 1 mL aliquots were digested with 1 mL of aqua regia (HCl/HNO_3, 3:1, v/v), and analyzed for total Au content by conventional ICP-MS.

Total Au Uptake in Nematode Samples. Total Au concentrations were measured in lyophilized control and exposed nematode samples after acid-assisted microwave digestion. Samples (≈2.0 mg of nematode or 1 mL of deionized water (calibration blank)) were weighed into prerinsed aluminum mini cups (≈18.0 mg). The cups were sealed by pressing them closed and then transferred into Teflon vessels with the addition of 7 mL of concentrated HNO_3 (Fisher Scientific Optima grade) and 3 mL of HCl (30−35%, Veritas grade, double-distilled). Samples were digested using a Mars Xpress microwave system under the following temperature programs: ramped to 180 °C over 15 min and then held at 180 °C for 20 min. The vessels were allowed to vent for 20 min, and the digests were quantitatively transferred to preweighed narrow-mouth low density polyethylene plastic bottles with an additional 10 mL of 1.5% (volume fraction) HNO_3. A 2 mL portion of this mixture was then diluted to 15 mL with an internal standard solution containing platinum (NIST SRM 3140) and indium (NIST SRM 3124a) in 2% (volume fraction) HNO_3. Calibration blanks and Au calibration standards (NIST SRM 3121: Gold (Au) Standard Solution) were prepared by serial dilution with the indium internal standard. Calibration blanks (10 in total), calibration standards, and sample digestions were analyzed by ICP-MS under the following conditions: 90 s sample uptake; five replicate measurements at m/z 115, 195, and 197; 0.45 mL/min flow rate.

Extraction of AuNPs from Biological Tissue. In order to liberate ingested particles from the nematodes, 0.1 mg samples of lyophilized nematodes were treated with 1 mL of 7% (w/w) TMAH; this TMAH concentration was optimized from preliminary experiments that examined the capacity of a range of TMAH concentrations to fully dissolve the nematodes yet not impact the size distribution of the AuNPs (complete details are provided in the Supporting Information). Samples were vortexed for 30 s and then allowed to digest at room temperature for 2 h. After 2 h, the samples were diluted with deionized water by a factor of $\approx 6 \times 10^5$ and bath-sonicated for 4 min for the detection of single particle events by spICP-MS.

TMAH Treatment of AuNPs. To test the effect of the TMAH digestion on the AuNP size distribution, a parallel study was performed to mimic the conditions of the TMAH digestion in the presence of biological material. AuNPs were treated with a TMAH concentration corresponding to the dilution factor utilized for lyophilized nematode samples, vortexed for 30 s, allowed to digest at room temperature for 2 h, diluted with deionized water, bath-sonicated for 4 min, and measured by spICP-MS. Further optimization of this strategy is described in the Supporting Information.

spICP-MS for AuNP Characterization. Single particle ICP-MS measurements of all samples were conducted using a Thermo Fisher X series VII quadrupole ICP-MS system (Waltham, MA, USA) with a C-type nebulizer (0.5 mL/min) and an impact bead spray chamber cooled to 2 °C. The instrument was tuned daily to a minimum $^{156}CeO/^{140}Ce$ oxide level (<2%) and a maximum ^{115}In sensitivity. The sample flow rate was set to approximately 0.45 mL/min, and the uptake rate was measured daily, in triplicate, by weighing the water uptake after 5 min of aspiration. AuNP suspensions were prepared by serial dilution of stock suspensions with deionized water to an approximate particle number concentration of 15 000 particles/mL. The instrument was calibrated using a blank (deionized water) and at least five soluble Au standards ranging from 0 to 10 ng/g Au in a thiourea solution (0.1% thiourea (w/v), 2.4% HCl (v/v), and 0.5% HNO_3 (v/v)). For the parallel study, all dissolved standards and AuNP suspensions were prepared in 0.07% TMAH (w/w) to compensate for possible matrix effects. A dwell time of 10 ms was selected for all spICP-MS measurements. For spICP-MS measurements of AuNPs, the signal for ^{197}Au was recorded using time-resolved analysis mode with Thermo Fisher PlasmaLab software. Data were exported to Microsoft Excel for data processing, wherein the transport efficiency was calculated using a method detailed by Pace *et al.*[55] Standard solutions were analyzed for 180 s, while AuNP suspensions and nematode digestions were measured three times for 360 s. All data were converted to counts/event and plotted against a time scale. A threshold of particle intensities five standard deviations above the mean signal intensity was chosen as the criteria for distinguishing between single particle events and the signal from dissolved ions in solution.[55−57] Particle sizes were calculated for all single particle events, and size distribution histograms were generated with a bin increment size of 1 nm.

High-Pressure Freezing/Freeze Substitution of Nematode Samples. Nematode samples in the 30 nm HEx and 60 nm LEx exposure conditions were resuspended in 20% bovine serum albumin (w/v) and cryo-immobilized by high-pressure freezing on gold carriers

DOI: 10.1021/acsnano.6b06582
ACS Nano 2017, 11, 526−540

(EMPact 2, Leica Microsystems GmbH, Wetzlar, Germany). Subsequently, the nematodes were freeze-substituted with acetone in combination with 1% OsO_4 and 0.1% uranyl acetate for approximately 4 h following the quick freeze substitution method detailed by McDonald.[58] After the samples were washed with acetone, the specimens were gradually infiltrated in Spurr's resins at room temperature followed by polymerization at 60 °C overnight. Ultrathin sections of embedded samples were collected on uncoated copper grids for SEM imaging. The 500 nm thick sections of embedded samples were mounted on carbon-coated glass coverslips for large-area SEM imaging.

Scanning Electron Microscopy of Nematode Cuticles. SEM/EDS analysis on whole nematodes and ultrathin sections was conducted with a Nova NanoLab 600 focused ion beam scanning electron microscope (FIB SEM) (FEI Company, Hillsboro, OR) equipped with a 100 mm^2 XMax silicon drift detector (SDD) and AztecEnergy (Oxford Instruments, Abingdon, UK) EDS system. EDS analysis was conducted at 10 and 20 kV using a beam current of 16–24 nA to collect the elemental maps and spot analysis. SEM image analysis was performed on nematodes exposed to 30 nm AuNPs at 100 ng/mL and on nematodes exposed to 60 nm AuNPs at 333 ng/mL Au mass fraction. After exposure and removal of excess AuNPs (by both Scheme 1 and Scheme 2), the nematodes were pipetted onto 5 mm × 5 mm Si wafers in 2 μL aliquots. The wafers were allowed to dry under a hood over a 2 day period. Initially, SEM analysis of sucrose-rinsed samples was hampered by extensive precipitation (salt crystal formation from buffers and media; data not shown). Therefore, those wafers were dipped in deionized water for 30 s and dried. Based on this procedure, the salt crystals were removed.

For additional confirmation that AuNPs were located on the nematode cuticle, SEM analysis and the EDS measurements of the whole nematodes were conducted with a Helios NanoLab 660 FIB SEM (FEI Company, Hillsboro, OR) equipped with a 30 mm^2 octane SDD and TEAM (EDAX, Mahwah, NJ) EDS system. Imaging and EDS analysis were conducted at 5 kV and 0.8 nA electron beam conditions. Au nanoparticle imaging was performed at 0 and 15° stage tilts. Images were collected in secondary electron and backscattered electron (BSE) modes.

Large-Area Scanning Electron Microscopy of Microtomed Nematode Slices. Large-area SEM imaging/EDS analysis was performed using the same Helios NanoLab 660 FIB SEM EDS system described above. Large-area imaging of the thick sections was performed using an automated tile imaging application MAPS (FEI Company, Hillsboro, OR). MAPS enables an automated imaging of $N \times M$ image tiles at user-specified imaging conditions such as pixel resolution, pixel dwell time, and tile overlap. Multiple large-area image tile sets were collected from the thick sectioned nematode samples. BSE imaging with immersion mode at 5 kV with a beam current of 800 pA was used to facilitate the detection of AuNPs in the nematode cross sections. Horizontal field width of 6 μm (3 nm pixel resolution) was used for each SEM image tile. A typical tile set consisted of 50 rows (x) and 50 columns (y) of image tiles with 10% image overlap in the x and y directions. A pixel dwell time of 3 ms was used for a relatively robust signal-to-noise ratio. Images from each tile set were manually inspected for the occurrences of high intensity punctate features, and EDS spot analysis was performed on each of these candidate features to determine whether they were AuNPs. The EDS confirmation of elemental constituents was necessary because the resin-embedded nematodes were osmicated, and as a result, many of the lipid-rich cellular components exhibited similar contrast as AuNPs. The EDS analysis was performed at 5 kV with an 800 pA beam current for effective excitation of Au X-ray M-lines (Mα at 2.123 keV and Mβ at 2.204 keV).

Statistical Analysis. Microsoft Excel and GraphPad Prism 5.0 software were utilized for statistical analyses. Significant differences (95% confidence level, $p < 0.05$) between experimental conditions (water *versus* sucrose, 0 h *versus* 24 h exposure) were determined by Welch's unequal variances t test. The F tests (95% confidence level, $p < 0.05$) were performed on the compared conditions to determine if they had significant (unequal) variances. All data are expressed as mean ±1 standard deviation (SD).

ASSOCIATED CONTENT

Supporting Information

The Supporting Information is available free of charge on the ACS Publications website at DOI: 10.1021/acsnano.6b06582.

Optimization of TMAH digestion of AuNPs and biological tissue; equations for the estimation of cuticle-adsorbed AuNPs and ingested AuNPs per *C. elegans*; relative % Au found in gradient layers following centrifugation of a mixture of 30 and 60 nm AuNPs at 100 ng mL^{-1} (Table S1), following a 0 h nematode exposure to a mixture of 30 and 60 nm AuNPs at 100 ng mL^{-1} (Table S2), and following a 24 h nematode exposure to 60 nm AuNPs at 333 ng mL^{-1} (Table S3); spICP-MS size distribution and representative ^{197}Au time-resolved data of 60 nm AuNPs (Figure S1); SEM image of a nematode exposed to 60 nm AuNPs following sample processing by Scheme 1 and complementary EDS spectra (Figure S2); 0 and 15° stage-tilted SEM images and complementary EDS spectrum of a nematode exposed to 60 nm AuNPs following sample processing by Scheme 1 (Figure S3); construction of the layers of the sucrose density gradient within the test tube (Figure S4); distribution of Au from sucrose density gradient centrifugal separation of a mixture of 30 and 60 nm AuNPs in the absence and presence of *C. elegans* (Figure S5); spICP-MS size distribution and representative ^{197}Au time-resolved data of 30 nm AuNPs (Figure S6); spICP-MS size distribution for 30 and 60 nm AuNPs in water and after TMAH digestion (Figure S7); large-area SEM image of nematodes exposed to 60 nm AuNPs (LEx) and processed *via* Scheme 2 (Figures S8 and S10); and large-area SEM image of nematodes exposed to 30 nm AuNPs (HEx) and processed *via* Scheme 2 (Figure S9) (PDF)

AUTHOR INFORMATION

Corresponding Authors

*E-mail: monique.johnson@nist.gov.

*E-mail: bryant.nelson@nist.gov.

ORCID

Monique E. Johnson: 0000-0001-5096-2003

Present Address

⊥A.L. and A.C.J.: The University of Maryland, College Park, Maryland 20742, United States.

Notes

Certain commercial equipment, instruments, and materials are identified in this paper to specify an experimental procedure as completely as possible. In no case does the identification of particular equipment or materials imply a recommendation or endorsement by the National Institute of Standards and Technology nor does it imply that the materials, instruments, or equipment are necessarily the best available for the purpose. The authors declare no competing financial interest.

ACKNOWLEDGMENTS

The authors thank Ru-Ching Hsia (University of Maryland, Baltimore) for unpublished micrographs and extensive optimization of *C. elegans* cryo-freezing; Bryce Marquis (University of Arkansas for Medical Sciences), Leona Scanlan

(California EPA Department of Pesticide Regulation), Sanem Hosbas Coskun (NIST), and Piper Hunt (Food and Drug Administration) for aid in *C. elegans* culturing; Scott Wight (NIST) for the use of the FIB/SEM instrument; Alexander Tona (NIST), Laura Wood (NIST), Terrie Butler (NIST), Susan Tai (NIST), Pawel Jaruga (NIST), and Erdem Coskun (NIST) for the use of equipment and supplies; and Savelas Rabb (NIST), Julian Tyson (University of Massachusetts Amherst), Hind El Hadri (NIST), Anne Galyean (Colorado School of Mines), Diana Ortiz-Montalvo (NIST), and Kathryn Riley (Swarthmore College) for helpful and thoughtful suggestions. S.K.H. and C.M.S. acknowledge funding and support from the National Academy of Sciences–National Research Council Postdoctoral Research Associateship Program. This work utilized a high-pressure freezer that was purchased with funding from a National Institutes of Health SIG grant (1S10RR26870-1) awarded to University of Maryland Baltimore. *C. elegans* nematodes (N2 Bristol strain) and *E. coli* were provided by the Caenorhabditis Genetics Center (CGC, University of Minnesota) which is funded by the NIH Office of Research Infrastructure Programs (P40 OD010440). The authors acknowledge the NIST SURF Program and the Montgomery College Internship Program, two of NIST's student educational programs that funded the research opportunities for A.L. and A.C.J.

REFERENCES

(1) Petersen, E. J.; Diamond, S. A.; Kennedy, A. J.; Goss, G. G.; Ho, K.; Lead, J.; Hanna, S. K.; Hartmann, N. B.; Hund-Rinke, K.; Mader, B.; Manier, N.; Pandard, P.; Salinas, E. R.; Sayre, P. Adapting OECD Aquatic Toxicity Tests for Use with Manufactured Nanomaterials: Key Issues and Consensus Recommendations. *Environ. Sci. Technol.* **2015**, *49*, 9532–9547.

(2) Petersen, E. J.; Henry, T. B.; Zhao, J.; MacCuspie, R. I.; Kirschling, T. L.; Dobrovolskaia, M. A.; Hackley, V.; Xing, B.; White, J. C. Identification and Avoidance of Potential Artifacts and Misinterpretations in Nanomaterial Ecotoxicity Measurements. *Environ. Sci. Technol.* **2014**, *48*, 4226–4246.

(3) Wiesner, M. R.; Lowry, G. V.; Alvarez, P.; Dionysiou, D.; Biswas, P. Assessing the Risks of Manufactured Nanomaterials. *Environ. Sci. Technol.* **2006**, *40*, 4336–4345.

(4) Mohan, N.; Chen, C. S.; Hsieh, H. H.; Wu, Y. C.; Chang, H. C. *In vivo* Imaging and Toxicity Assessments of Fluorescent Nanodiamonds in *Caenorhabditis elegans*. *Nano Lett.* **2010**, *10*, 3692–3699.

(5) Brenner, S. The Genetics of *Caenorhabditis elegans*. *Genetics* **1974**, *77*, 71–94.

(6) Huguier, P.; Manier, N.; Meline, C.; Bauda, P.; Pandard, P. Improvement of the *Caenorhabditis elegans* Growth and Reproduction Test to Assess the Ecotoxicity of Soils and Complex Matrices. *Environ. Toxicol. Chem.* **2013**, *32*, 2100–2108.

(7) Hulme, S. E.; Whitesides, G. M. Chemistry and the Worm: *Caenorhabditis elegans* as a Platform for Integrating Chemical and Biological Research. *Angew. Chem., Int. Ed.* **2011**, *50*, 4774–4807.

(8) Bischof, L. J.; Huffman, D. L.; Aroian, R. V. Assays for Toxicity Studies in *C. elegans* with Bt Crystal Proteins. In *C. elegans: Methods and Applications*; Strange, K., Ed.; Humana Press: Totowa, NJ, 2006; pp 139–154.

(9) Hoss, S.; Ahlf, W.; Bergtold, M.; Bluebaum-Gronau, E.; Brinke, M.; Donnevert, G.; Menzel, R.; Mohlenkamp, C.; Ratte, H. T.; Traunspurger, W.; von Danwitz, B.; Pluta, H. J. Interlaboratory Comparison of a Standardized Toxicity Test Using the Nematode *Caenorhabditis elegans* (ISO 10872). *Environ. Toxicol. Chem.* **2012**, *31*, 1525–1535.

(10) Kaletta, T.; Hengartner, M. O. Finding Function in Novel Targets: *C. elegans* as a Model Organism. *Nat. Rev. Drug Discovery* **2006**, *5*, 387–398.

(11) Hunt, P. R. The *C. elegans* Model in Toxicity Testing. *J. Appl. Toxicol.* **2017**, *37*, 50–39.

(12) Ma, H.; Bertsch, P. M.; Glenn, T. C.; Kabengi, N. J.; Williams, P. L. Toxicity of Manufactured Zinc Oxide Nanoparticles in the Nematode *Caenorhabditis elegans*. *Environ. Toxicol. Chem.* **2009**, *28*, 1324–1330.

(13) Wang, H.; Wick, R. L.; Xing, B. Toxicity of Nanoparticulate and Bulk ZnO, Al_2O_3 and TiO_2 to the Nematode *Caenorhabditis elegans*. *Environ. Pollut.* **2009**, *157*, 1171–1177.

(14) Gao, Y.; Liu, N. Q.; Chen, C. Y.; Luo, Y. F.; Li, Y. F.; Zhang, Z. Y.; Zhao, Y. L.; Zhao, B. L.; Iida, A.; Chai, Z. F. Mapping technique for Biodistribution of Elements in a Model Organism, *Caenorhabditis elegans*, after Exposure to Copper Nanoparticles with Microbeam Synchrotron Radiation X-ray Fluorescence. *J. Anal. At. Spectrom.* **2008**, *23*, 1121–1124.

(15) Hunt, P. R.; Marquis, B. J.; Tyner, K. M.; Conklin, S.; Olejnik, N.; Nelson, B. C.; Sprando, R. L. Nanosilver Suppresses Growth and Induces Oxidative Damage to DNA in *Caenorhabditis elegans*. *J. Appl. Toxicol.* **2013**, *33*, 1131–1142.

(16) Yang, X.; Jiang, C.; Hsu-Kim, H.; Badireddy, A. R.; Dykstra, M.; Wiesner, M.; Hinton, D. E.; Meyer, J. N. Silver Nanoparticle Behavior, Uptake, and Toxicity in *Caenorhabditis elegans*: Effects of Natural Organic Matter. *Environ. Sci. Technol.* **2014**, *48*, 3486–3495.

(17) Hoss, S.; Fritzsche, A.; Meyer, C.; Bosch, J.; Meckenstock, R. U.; Totsche, K. U. Size- and Composition-dependent Toxicity of Synthetic and Soil-derived Fe oxide Colloids for the Nematode *Caenorhabditis elegans*. *Environ. Sci. Technol.* **2015**, *49*, 544–552.

(18) Kim, S. W.; Kwak, J. I.; An, Y. J. Multigenerational Study of Gold Nanoparticles in *Caenorhabditis elegans*: Transgenerational Effect of Maternal Exposure. *Environ. Sci. Technol.* **2013**, *47*, 5393–5399.

(19) Selck, H.; Handy, R. D.; Fernandes, T. F.; Klaine, S. J.; Petersen, E. J. Nanomaterials in the Aquatic Environment: A European Union–United States Perspective on the Status of Ecotoxicity Testing, Research Priorities, and Challenges Ahead. *Environ. Toxicol. Chem.* **2016**, *35*, 1055–1067.

(20) Benn, T. M.; Westerhoff, P. Nanoparticle Silver Released into Water from Commercially Available Sock Fabrics. *Environ. Sci. Technol.* **2008**, *42*, 4133–4139.

(21) Geranio, L.; Heuberger, M.; Nowack, B. The Behavior of Silver Nanotextiles During Washing. *Environ. Sci. Technol.* **2009**, *43*, 8113–8118.

(22) Gondikas, A. P.; von der Kammer, F.; Reed, R. B.; Wagner, S.; Ranville, J. F.; Hofmann, T. Release of TiO_2 Nanoparticles from Sunscreens into Surface Waters: A One-year Survey at the Old Danube Recreational Lake. *Environ. Sci. Technol.* **2014**, *48*, 5415–5422.

(23) Reed, R. B.; Goodwin, D. G.; Marsh, K. L.; Capracotta, S. S.; Higgins, C. P.; Fairbrother, D. H.; Ranville, J. F. Detection of Single Walled Carbon Nanotubes by Monitoring Embedded Metals. *Env. Sci. Process. Impact.* **2013**, *15*, 204–213.

(24) Windler, L.; Lorenz, C.; von Goetz, N.; Hungerbuhler, K.; Amberg, M.; Heuberger, M.; Nowack, B. Release of Titanium Dioxide from Textiles During Washing. *Environ. Sci. Technol.* **2012**, *46*, 8181–8188.

(25) Degueldre, C.; Favarger, P. Y. Colloid Analysis by Single Particle Inductively Coupled Plasma-mass Spectroscopy: A Feasibility Study. *Colloids Surf., A* **2003**, *217*, 137–142.

(26) Degueldre, C.; Favarger, P. Y. Thorium Colloid Analysis by Single Particle Inductively Coupled Plasma-mass Spectrometry. *Talanta* **2004**, *62*, 1051–1054.

(27) Degueldre, C.; Favarger, P. Y.; Bitea, C. Zirconia Colloid Analysis by Single Particle Inductively Coupled Plasma-mass Spectrometry. *Anal. Chim. Acta* **2004**, *518*, 137–142.

(28) Degueldre, C.; Favarger, P. Y.; Wold, S. Gold Colloid Analysis by Inductively Coupled Plasma-mass Spectrometry in a Single Particle Mode. *Anal. Chim. Acta* **2006**, *555*, 263–268.

(29) Montoro Bustos, A. R.; Petersen, E. J.; Possolo, A.; Winchester, M. R. *Post hoc* Interlaboratory Comparison of Single Particle ICP-MS Size Measurements of NIST Gold Nanoparticle Reference Materials. *Anal. Chem.* **2015**, *87*, 8809–8817.

DOI: 10.1021/acsnano.6b06582
ACS Nano 2017, 11, 526–540

(30) Scanlan, L. D.; Reed, R. B.; Loguinov, A. V.; Antczak, P.; Tagmount, A.; Aloni, S.; Nowinski, D. T.; Luong, P.; Tran, C.; Karunaratne, N.; Pham, D.; Lin, X. X.; Falciani, F.; Higgins, C. P.; Ranville, J. F.; Vulpe, C. D.; Gilbert, B. Silver Nanowire Exposure Results in Internalization and Toxicity to *Daphnia magna*. *ACS Nano* **2013**, *7*, 10681−10694.
(31) Dan, Y.; Zhang, W.; Xue, R.; Ma, X.; Stephan, C.; Shi, H. Characterization of Gold Nanoparticle Uptake by Tomato Plants Using Enzymatic Extraction followed by Single Particle Inductively Coupled Plasma-mass Spectrometry Analysis. *Environ. Sci. Technol.* **2015**, *49*, 3007−3014.
(32) Peters, R. J.; Rivera, Z. H.; van Bemmel, G.; Marvin, H. J.; Weigel, S.; Bouwmeester, H. Development and Validation of Single Particle ICP-MS for Sizing and Quantitative Determination of Nano-silver in Chicken Meat. *Anal. Bioanal. Chem.* **2014**, *406*, 3875−3885.
(33) Gray, E.; Higgins, C. P.; Ranville, J. F. Analysis of Nanoparticles in Biological Tissues Using sp-ICP-MS; http://www.perkinelmer.com/CMSResources/Images/44-161572APP_NexION-350Q-Silver-Nanoparticles-in-Bio-Tissues-011803_01.pdf, 2014 (Accessed September 11, 2015).
(34) Gray, E. P.; Coleman, J. G.; Bednar, A. J.; Kennedy, A. J.; Ranville, J. F.; Higgins, C. P. Extraction and Analysis of Silver and Gold Nanoparticles from Biological Tissues Using Single Particle Inductively Coupled Plasma Mass Spectrometry. *Environ. Sci. Technol.* **2013**, *47*, 14315−14323.
(35) Johnstone, I. L. The cuticle of the nematode *Caenorhabditis elegans*: A complex collagen structure. *BioEssays* **1994**, *16*, 171−178.
(36) Kumar, S. A.; Peter, Y. A.; Nadeau, J. *Biosynthesis, Separation and Conjugation of Gold Nanoparticles to Doxorubicin for Cellular Uptake and Toxicity*; IEEE: New York, 2009; pp 5−12.
(37) Lee, S. H.; Salunke, B. K.; Kim, B. S. Sucrose Density Gradient Centrifugation Separation of Gold and Silver Nanoparticles Synthesized Using *Magnolia kobus* Plant Leaf Extracts. *Biotechnol. Bioprocess Eng.* **2014**, *19*, 169−174.
(38) Xiong, B.; Cheng, J.; Qiao, Y.; Zhou, R.; He, Y.; Yeung, E. S. Separation of Nanorods by Density Gradient Centrifugation. *J. Chromatogr. A* **2011**, *1218*, 3823−3829.
(39) Reina, A.; Subramaniam, A. B.; Laromaine, A.; Samuel, A. D. T.; Whitesides, G. M. Shifts in the Distribution of Mass Densities Is a Signature of Caloric Restriction in *Caenorhabditis elegans*. *PLoS One* **2013**, *8*, e69651.
(40) Lewis, J. A.; Fleming, J. T. *Methods in Cell Biolgy: Caenorhabditis elegans: Modern Biological Analysis of an Organism*; Elsevier: Amsterdam, 1995; Vol. *48*, pp 4−29.
(41) Stiernagle, T. *C. elegans*: A Practical Approach; http://www.wormbook.org/chapters/www_strainmaintain/strainmaintain.pdf, pp 51−67 (Accessed September 14, 2015).
(42) Meyer, J. N.; Lord, C. A.; Yang, X. Y.; Turner, E. A.; Badireddy, A. R.; Marinakos, S. M.; Chilkoti, A.; Wiesner, M. R.; Auffan, M. Intracellular Uptake and Associated Toxicity of Silver Nanoparticles in *Caenorhabditis elegans*. *Aquat. Toxicol.* **2010**, *100*, 140−150.
(43) Kim, S. W.; Nam, S. H.; An, Y. J. Interaction of Silver Nanoparticles with Biological Surfaces of *Caenorhabditis elegans*. *Ecotoxicol. Environ. Saf.* **2012**, *77*, 64−70.
(44) Arnold, M. C.; Badireddy, A. R.; Wiesner, M. R.; Di Giulio, R. T.; Meyer, J. N. Cerium Oxide Nanoparticles are More Toxic than Equimolar Bulk Cerium Oxide in *Caenorhabditis elegans*. *Arch. Environ. Contam. Toxicol.* **2013**, *65*, 224−233.
(45) Maurer, L. L.; Yang, X.; Schindler, A. J.; Taggart, R. K.; Jiang, C.; Hsu-Kim, H.; Sherwood, D. R.; Meyer, J. N. Intracellular Trafficking Pathways in Silver Nanoparticle Uptake and Toxicity in *Caenorhabditis elegans*. *Nanotoxicology* **2016**, *10*, 831−835.
(46) Report of Investigation for Reference Material 8012, Gold Nanoparticles, Nominal 30 nm Diameter, 2012.
(47) Report of Investigation for Reference Material 8013, Gold Nanoparticles, Nominal 60 nm Diameter, 2012.
(48) Mahapatra, I.; Sun, T. Y.; Clark, J. R. A.; Dobson, P. J.; Hungerbuehler, K.; Owen, R.; Nowack, B.; Lead, J. Probabilistic Modelling of Prospective Environmental Concentrations of Gold Nanoparticles from Medical Applications as a Basis for Risk Assessment. *J. Nanobiotechnol.* **2015**, *13*, 1−14.
(49) Weber, K. P.; Petersen, E. J.; Bissegger, S.; Koch, I.; Zhang, J.; Reimer, K. J.; Rehmann, L.; Slawson, R. M.; Legge, R. L.; O'Carroll, D. M. Effect of gold nanoparticles and ciprofloxacin on microbial catabolism: a community-based approach. *Environ. Toxicol. Chem.* **2014**, *33*, 44−51.
(50) Johnson, M. E.; Montoro Bustos, A. R.; Winchester, M. R. Practical Utilization of spICP-MS to Study Sucrose Density Gradient Centrifugation for the Separation of Nanoparticles. *Anal. Bioanal. Chem.* **2016**, *408*, 7629−7640.
(51) Montoro Bustos, A. R.; Purushotham, K.; Vladar, A.; Murphy, K. E.; Winchester, M. R. Matrix Effects and Validation of Single Particle Icp-Ms for Measuring Nanoparticle Size and Size Distribution. In *Proceedings of the Winter Conference on Plasma Spectrochemistry*; January 11−16, 2016, Tuscon, AZ.
(52) Chauhan, V. M.; Orsi, G.; Brown, A.; Pritchard, D. I.; Aylott, J. W. Mapping the Pharyngeal and Intestinal pH of *Caenorhabditis elegans* and Real-time Luminal pH Oscillations Using Extended Dynamic Range pH-sensitive Nanosensors. *ACS Nano* **2013**, *7*, 5577−5587.
(53) Hall, D. H.; Altun, Z. F. *C. elegans Altlas*; Cold Spring Harbor Laboratory Press, 2008
(54) Lee, S.; Bi, X.; Reed, R. B.; Ranville, J. F.; Herckes, P.; Westerhoff, P. Nanoparticle Size Detection Limits by Single Particle ICP-MS for 40 Elements. *Environ. Sci. Technol.* **2014**, *48*, 10291−10300.
(55) Pace, H. E.; Rogers, N. J.; Jarolimek, C.; Coleman, V. A.; Higgins, C. P.; Ranville, J. F. Determining Transport Efficiency for the Purpose of Counting and Sizing Nanoparticles *via* Single Particle Inductively Coupled Plasma Mass Spectrometry. *Anal. Chem.* **2011**, *83*, 9361−9369.
(56) Liu, J.; Murphy, K. E.; MacCuspie, R. I.; Winchester, M. R. Capabilities of Single Particle Inductively Coupled Plasma Mass Spectrometry for the Size Measurement of Nanoparticles: A Case Study on Gold Nanoparticles. *Anal. Chem.* **2014**, *86*, 3405−3414.
(57) Tuoriniemi, J.; Cornelis, G.; Hassellöv, M. Size Discrimination and Detection Capabilities of Single Particle ICPMS for Environmental Analysis of Silver Nanoparticles. *Anal. Chem.* **2012**, *84*, 3965−3972.
(58) McDonald, K. L. Out with the Old and in with the New: Rapid Specimen Preparation Procedures for Electron Microscopy of Sectioned Biological Material. *Protoplasma* **2014**, *251*, 429−448.

DOI: 10.1021/acsnano.6b06582
ACS Nano 2017, 11, 526−540